Regulation of defective mitochondrial DNA accumulation and transmission in *C. elegans* by the programmed cell death and aging pathways

4   Sagen E. Flowers[1], Rushali Kothari[1], Yamila N. Torres Cleuren[1,2], Melissa R. Alcorn[1], Chee Kiang

5   Ewe[1], Geneva Alok[1], Pradeep M. Joshi[1], Joel H. Rothman[1]

6   Affiliations:

7   1. Department of MCD Biology and Neuroscience Research Institute, University of

8   California Santa Barbara, CA, USA

9   2. Computational Biology Unit, Institute for Informatics, University of Bergen, Norway

10   To whom correspondence should be addressed: rothman@lifesci.ucsb.edu

11   Keywords: heteroplasmy, uaDf5, purifying selection, programmed cell death, aging, insulin

12   signaling

13   ORCiD:

14   SEF - 0000-0002-7818-2188

15   RK - 000-0001-7220-932X

16   YNTC- 0000-0003-2218-7243

17   MRA- 0000-0001-6284-3255

18   CKE - 0000-0003-1973-1308

19   GA- 0000-0001-6257-2344

20   PMJ- 0000-0002-4220-0559

21   JHR - 0000-0002-6844-1377

22

Abstract

The heteroplasmic state of eukaryotic cells allows for cryptic accumulation of defective mitochondrial genomes (mtDNA). "Purifying selection" mechanisms operate to remove such dysfunctional mtDNAs. We found that activators of programmed cell death (PCD), including the CED-3 and CSP-1 caspases, the BH3-only protein CED-13, and PCD corpse engulfment factors, are required in *C. elegans* to attenuate germline abundance of a 3.1 kb mtDNA deletion mutation, *uaDf5*, which is normally stably maintained in heteroplasmy with wildtype mtDNA. In contrast, removal of CED-4/Apaf1 or a mutation in the CED-4-interacting prodomain of CED-3, do not increase accumulation of the defective mtDNA, suggesting induction of a non-canonical germline PCD mechanism or non-apoptotic action of the CED-13/caspase axis. We also found that the abundance of germline mtDNA^{uaDf5} reproducibly increases with age of the mothers. This effect is transmitted to the offspring of mothers, with only partial intergenerational removal of the defective mtDNA. In mutants with elevated mtDNA^{uaDf5} levels, this removal is enhanced in older mothers, suggesting an age-dependent mechanism of mtDNA quality control. Indeed, we found that both steady-state and age-dependent accumulation rates of *uaDf5* are markedly decreased in long-lived, and increased in short-lived, mutants. These findings reveal that regulators of both PCD and the aging program are required for germline mtDNA quality control and its intergenerational transmission.

42 **Introduction**

43   Mitochondrial diseases are a group of conditions that affect mitochondrial functions in

44 up to 1 in 4,300 people [1–3]. Generally, these diseases present as dysfunction in the tissues or

45 organs with the most intensive energy demands, most commonly in muscle and the nervous

46 system [4]. Many of these diseases are attributable to mutations in the mitochondrial DNA

47 (mtDNA) or nuclear DNA (nDNA), and include those disorders with defects in mitochondrial

48 function, dynamics, or quality control, or in which there is miscommunication between the

49 mitochondria and the endoplasmic reticulum (ER) [3,5]. The progressive advancement of the

50 diseased state resulting from age-dependent accumulation of mutant mtDNA is a common trait

51 among mitochondrial diseases [6–8]. While the severity of the disease varies with the nature of

52 the mutation, the most severe phenotypes result in childhood death, as in Leigh syndrome and

53 MELAS [5,9]. As there are currently no pharmacological treatments for mitochondrial diseases, it

54 is of great importance to uncover the cellular processes that underlie the regulation of mtDNA

55 quality control.

56   mtDNAs show high mutation rates [10–12] and hence it is critical that cells possess

57 mechanisms to remove detrimental mtDNA alleles, a process called purifying selection [13,14].

58 Defects in this process can result in mitochondrial diseases, allowing harmful mtDNA mutations

59 to persist through the maternal germline and subsequent generations. Processes that regulate

60 mtDNA quality control include mitochondrial fission/fusion dynamics and mitophagy [8,15–20],

61 and the mitochondrial unfolded protein response (UPR^{MT}; [21–27]. Further, it has also been

62 found that the insulin/IGF-1 signaling pathway (IIS; [28,29]) ameliorates the fitness defects of

63 mutant mtDNA.

4

64   One potential cellular process that could be used to eliminate defective mtDNAs is the

65   culling of cells bearing mtDNA mutations by programmed cell death (PCD). The mechanisms of

66   both developmentally controlled and genotoxicity-induced PCD have been shown to be well-

67   conserved across metazoans [30], and much of the machinery that choreographs this process is

68   directed by mitochondria [31–33]. Mitochondrial-dependent processes participating in PCD

69   include permeabilization of the inner mitochondrial membrane and release of mitochondrial

70   factors that mediate transduction of intermediary events in the cell suicide program [31–33].

71   Both mitochondrial function and PCD are linked to the process of organismal aging [34]. mtDNA

72   mutations accumulate in tissues as organisms age, and it has been suggested that this

73   accumulation is a major contributor to aging [35–37].

74   The nematode *C. elegans* provides an attractive model for exploring the potential role of

75   PCD in mtDNA purifying selection. The well-described, conserved PCD regulatory pathway in *C.*

76   *elegans* functions not only to eliminate 131 somatic cells during development through a rigidly

77   stereotyped program [38], but is also activated apparently stochastically during germline

78   development, resulting in the death of >95% of nuclei that would otherwise be destined to

79   become oocytes in the mature hermaphrodite [30,39–41]. In addition to this "physiological" PCD,

80   germline nuclei that have experienced genotoxic stress are eliminated through p53-dependent

81   apoptosis, as is also the case in somatic mammalian cells [42,43]. Thus, germline PCD allows for

82   selective removal of nuclei with damaged genomes, thereby preventing intergenerational

83   transmission of defective nuclear DNA. Given the prominent role played by mitochondria in the

84   PCD process, it is conceivable that mitochondrial dysfunction could trigger PCD in the germline

85   and, as such, might similarly provide a quality control mechanism for eliminating aberrant

86   mtDNA, as seen for the nuclear genome.

87   We report here that germline mtDNA quality control in *C. elegans* is influenced by

88   regulators of both PCD and the aging program. We find that pro-apoptotic regulators of germline

89   PCD, notably the caspases CED-3 and CSP-1, the BH3-only domain protein CED-13, and regulators

90   of cell corpse engulfment, reduce abundance of an mtDNA deletion and that abrogation of their

91   functions results in elevated levels of the defective mtDNA. Notably, however, loss of the CED-3

92   activator CED-4/Apaf1 [44,45] does not result in elevated levels of defective mtDNA. These

93   findings raise the possibilities that either the caspases and the other pro-apoptotic factors

94   function in mtDNA purifying selection by a non-canonical CED-4-independent cell death program,

95   or that these pro-apoptotic regulators function in mtDNA purifying selection through a PCD-

96   independent mechanism. We also report that defective mtDNA accumulates in the germline of

97   animals with age and that although the abundance of the defective mtDNA is reduced in

98   offspring, progeny of older mothers inherit higher levels of the mutant mtDNA than those from

99   young mothers. Intergenerational removal of the defective mtDNA appears to be enhanced in

100   older animals with defective mtDNA quality control. Further, we found that lifespan-extending

101   mutations in both the IIS pathway and the non-IIS-dependent lifespan-regulator CLK-1/MCLK1

102   decrease accumulation of defective mtDNA, and that short-lived mutants show elevated

103   accumulation, implicating molecular regulators of the aging process in mtDNA purifying

104   selection. Our findings reveal that the PCD machinery and the aging program contribute to the

105   removal of mtDNA mutations during germline development and their intergenerational

106   transmission.

107

6

108   **Results**

109   **The stably maintained mtDNA deletion mutant *uaDf5* contains multiple linked mutations**

110   **resulting in aberrant proteins and shows deleterious effects on growth**

111   To test the role of potential regulatory factors in mtDNA purifying selection, we took

112   advantage of *uaDf5*, a 3.1 kb mtDNA deletion mutation that removes part or all of four protein-

113   coding genes and seven tRNAs (Fig. 1A) [46]. Given the presumably deleterious nature of this

114   defective mtDNA, it was of interest to understand how it is stably transmitted despite active

115   purifying selection processes. While its maintenance at high levels is attributable in part to

116   stabilization by the mitochondrial UPR [25], *uaDf5* persists, albeit at lower levels, in animals

117   lacking this activity. One possible explanation for this phenomenon is that the mutant mtDNA

118   might be maintained in heteroplasmy with an otherwise intact mtDNA carrying a complementing

119   mutation. We sought to test this possibility through deep sequencing of mtDNA isolated from

120   the *uaDf5*-bearing strain. Comprehensive sequence analysis revealed that, in addition to the

121   large deletion, the strain indeed carries a second mtDNA mutation, *w47* (Fig. 1A, Fig. 1 – figure

122   supplement 1A, B, C). *w47* is a single base pair insertion in the *nduo-4* gene that causes a

123   frameshift, predicted to result in a truncated NADH dehydrogenase 4 (ND4) protein lacking 321

124   residues (Fig. 1 – figure supplement 1D). ND4 is an essential transmembrane subunit within

125   complex I of the mitochondrial respiratory chain (MRC), which drives NADH-oxidation-dependent

126   transport of protons across the inner mitochondrial membrane [47–49]. While this raised the

127   possibility of two complementing mtDNA genomes, we found that the *w47* mutation is present

128   at the same abundance as the *uaDf5* deletion mutation (~75% of total mtDNA, Fig. 1 – figure

129   supplement 1B) rather than that of the wild-type mtDNA, strongly suggesting that it resides on

7

130   the same mtDNA genome. As this second mutation cannot explain stabilization of the defective

131   mtDNA by *trans*-complementation of two deleterious mutations, other mechanisms appear to

132   promote the stable inheritance of *uaDf5*.

133   In addition to the aberrant protein encoded by the *w47* frameshift mutation in *nduo-4*, a

134   second abnormal protein is encoded by the *uaDf5* genome: one end of the deletion results in a

135   fusion protein comprised of the first 185 amino acids of NADH dehydrogenase 1 (ND1, a homolog

136   of the core MT-ND1 transmembrane subunit of complex I of the MRC [47,49,50]), and the last 81

137   amino acids of mitochondrial-encoded cytochrome b (CTB-1/CYTB, a transmembrane subunit of

138   complex III of the MRC [47,49,51]) (Fig. 1 – figure supplement 1E). It is conceivable that

139   accumulation of these two abnormal proteins -- the truncated ND4 and the ND1-CYTB fusion

140   protein resulting from *w47* and *uaDf5*, respectively – activate the UPR^{MT}, which has been shown

141   to result in clearance of mtDNA^{uaDf5}, dependent on the ATFS-1 transcription factor [25,27].

142   Animals harboring mtDNA^{uaDf5} are viable and fertile, presumably because they contain

143   intact wildtype mtDNA [46]. However, we found that *uaDf5*-bearing animals displayed a

144   significant reduction in brood size (WT 304 ± 4.8; *uaDf5* 201 ± 8.6 embryos laid, p < 0.001) (Fig.

145   1B) and a significant increase in embryonic lethality (WT 1.4 ± 0.2%; *uaDf5* 4.2 ± 0.7%, p < 0.001)

146   (Fig. 1C). Additionally, *uaDf5* animals are slow-growing, evident in both the number of hours to

147   reach gravidity (WT 63 ± 0.8; *uaDf5* 76 ± 1.4 hours at 20°C, p < 0.001) (Fig. 1D) and the stage of

148   development reached after 60 hours of feeding (WT: adult; *uaDf5:* mid-L4) (Fig. 1E). In contrast,

149   however, we were surprised to find that lifespan was not substantially affected (WT 14 ± 0.4;

150   *uaDf5* 15 ± 0.5 days) (Fig. 1F, Fig. 1 – figure supplement 2). Given the significant decline in the

151   majority of fitness parameters tested, we conclude that *uaDf5* is a useful tool for studying

152   mitochondrial disease and mechanisms underlying mtDNA quality control.

153   **PCD regulators promote removal of mtDNA*uaDf5***

154   During germline development in *C. elegans*, as many as 95% of nuclei destined to become

155   potential oocytes are eliminated by PCD [39–41,52]. While this process has been proposed to be

156   stochastically determined [39,52], it has also been suggested that it may function to selectively

157   remove all but the most "fit" germline cells. As such, PCD could perform a role in purifying

158   selection in the germline, wherein potential oocytes that undergo PCD are associated with higher

159   levels of defective mtDNA. To test this hypothesis, we introduced *uaDf5* into various PCD mutants

160   and quantified abundance of the defective mtDNA by digital-droplet PCR (ddPCR; see

161   Supplementary Table 1 for list of mutants tested). In a wildtype genetic background, we found

162   that the steady-state fractional abundance of *uaDf5* in populations of 200 day 1 adults (first day

163   of adulthood) is highly reproducible across four separate trials, demonstrating the reliability and

164   robustness of the assay. Our analyses confirmed that mtDNA*uaDf5* constitutes the major molar

165   fraction of mtDNA in the *uaDf5*-bearing strain by a nearly 3:1 ratio (Fig. 2 – figure supplement 1).

166   CED-3 in *C. elegans* is the major executioner caspase in the canonical PCD pathway

167   [38,52,53] and is required for virtually all PCD both in the germline and the soma (Fig. 2 – figure

168   supplement 2). We found that two *ced-3* mutations that strongly block PCD [54] showed a

169   significant increase in the ratio of defective to normal mtDNA from a molar ratio of 2.9:1 for *ced-*

170   *3(+)* to 3.5:1 for *ced-3(n717)* and 4.6:1 for *ced-3(n1286)* (Fig. 2A). This effect appears to be

171   exclusively attributable to an increase in mtDNA*uaDf5* in the PCD-deficient strains, as the

172   abundance of mtDNA^{WT} is not significantly different between the strains. These *ced-3(-)*

9

173 mutations both localize to the p15 domain of the protease portion of CED-3 (Fig. 2 – figure

174 supplement 3), consistent with abolition of caspase activity. These findings implicate the CED-3

175 caspase and its p15 domain in mtDNA quality control. We found that one other mutation located

176 in the p15 domain showed only a very slight increase that was not statistically significant (*n2454:*

177 2.9:1, Fig. 2B). While it is unclear why this allele showed a weaker effect it is noteworthy that,

178 unlike the other two mutations, which result in a dramatic alteration of the protein, this mutation

179 is predicted to result in a relatively modest (ala → thr) single amino acid substitution.

180 A second caspase in *C. elegans*, CSP-1, also functions, albeit less prominently, in PCD.

181 While loss of CSP-1 alone does not result in a strong reduction in PCD, it synergizes with loss of

182 CED-3 both in PCD and in other caspase-dependent processes (Fig. 2 – figure supplement 2) [55–

183 57]. We found that removing CSP-1 in the *csp-1(tm917)* knockout mutant results in a significant

184 increase in mtDNA^{uaDf5} abundance to a molar ratio of 3.9:1 (Fig. 2A). Further, we found that this

185 mutation enhances the effect of the *ced-3(n717)* mutation, increasing the mtDNA^{uaDf5}:mtDNA^{WT}

186 molar ratio from 3.5:1 to 4.7:1 (Fig. 2A). Together these findings demonstrate that caspase

187 activity, and possible PCD-mediated clearance, are crucial for mtDNA quality control and function

188 in purifying selection of defective mtDNA.

189 We sought to further investigate a potential role for PCD in mtDNA purifying selection by

190 evaluating the requirement for the pro-apoptotic factor CED-13, a BH3-only domain protein that

191 acts specifically in the germline to activate PCD [38,58,59]. Consistent with a requirement for PCD

192 in purifying selection, we found that two *ced-13* alleles result in a very substantial increase in the

193 mtDNA^{uaDf5}:mtDNA^{WT} molar ratio (*sv32*: 4.2:1 and *tm536*: 5.1:1) (Fig. 2A), supporting the notion

194 that CED-13 promotes removal of defective mtDNA in the germline. CED-13 functions in PCD by

195   antagonizing the function of mitochondrially localized CED-9/Bcl-2 [58,59], which normally

196   sequesters the apoptosome factor CED-4/APAF1 at mitochondria, thereby preventing it from

197   triggering autocatalytic conversion of the executioner caspase zymogen proCED-3 to its pro-

198   apoptotic protease structure (Fig. 2 – figure supplement 2) [60]. An equivalent action is carried

199   out in the soma by the BH3-only protein EGL-1 [60]. *n1950*, a gain-of-function allele of *ced-9* that

200   blocks the interaction of EGL-1 with CED-9 at the mitochondria, results in elimination of PCD in

201   the soma but not the germline [39,52,60,61]. Consistent with the lack of effect of *ced-9(n1950gf)*

202   on germline PCD, we found that the mtDNA^{uaDf5}:mtDNA^{WT} molar ratio was not increased in *ced-*

203   *9(n1950gf)* mutants (2.2:1) (Fig. 2B). Thus, CED-3, CSP-1, and CED-13 are required both for

204   germline PCD and for removal of mtDNA^{uaDf5}.

205   Cells that undergo PCD are cleared by the surrounding cells in the process of engulfment

206   and degradation, which is implemented through a set of redundant pathways that converge on

207   the CED-10 GTPase [62–65] (Fig. 2 – figure supplement 2). Although this engulfment process is

208   necessary primarily for removal of the resultant corpses, it also appears to play an active role in

209   cell killing: inhibition of the engulfment pathway diminishes occurrence of PCD, likely through a

210   complex feedback mechanism [66,67]. Further supporting a role for PCD in purifying selection,

211   we found that single or double mutations of several genes that promote engulfment of cell

212   corpses result in elevated mtDNA^{uaDf5}:mtDNA^{WT} molar ratios, ranging from 3.5:1 to 5.2:1 (4.1:1

213   for *ced-1(e1735)*, 4.5:1 for *ced-2(e1752)*, 5.2:1 for the *ced-1(e1735); ced-2(e1752)* double

214   mutant, 3.6:1 for *ced-10(n1993)*, and 4.8:1 for *ced-10(n3246)*; Fig. 2A).

215   We tested whether *generally* increased germline PCD alters mtDNA^{uaDf5} abundance by

216   examining the effect of removing the caspase-related factor, CSP-2, which has been shown to

11

217   play an anti-apoptotic role through inhibition of CED-3 autoactivation in the germline (Fig. 2 –

218   figure supplement 2) [68]. We found that a loss-of-function mutation in *csp-2*, which elevates

219   germline PCD, did not alter the mtDNA^{uaDf5}:mtDNA^{WT} molar ratio (2.9:1 for the *csp-2(tm3077)*

220   knockout mutation) (Fig. 2B). This observation does not conflict with a requirement for PCD in

221   purifying selection: a general increase in PCD in the germline of *csp-2(-)* animals would not be

222   expected *per se* to alter the mechanism that *discriminates* defective from normal mtDNAs and

223   therefore the relative abundance of the two forms. Rather, our findings suggest that the

224   mechanisms that recognizes and disposes of the defective mtDNA specifically requires PCD

225   components acting in a selective, rather than general process (i.e., in those cells with the highest

226   burden of the defective mtDNA).

227

228   **Evidence for non-canonical action of PCD regulators in mtDNA purifying selection**

229   The foregoing results implicate a role for the pro-apoptotic CED-3 and CSP-1 caspases,

230   CED-13, and the CED-1, 2, and -10 cell corpse engulfment factors in mtDNA purifying selection.

231   However, several observations suggest that elimination of normal, physiological germline PCD

232   *per se* is insufficient to increase accumulation of defective mtDNA, or that these factors promote

233   purifying selection through a PCD-independent pathway. Specifically, we observed that the

234   occurrence of PCD does not perfectly correlate with their effects on accumulation of mtDNA^{uaDf5}

235   in particular mutants.

236   First, we found that the *ced-3(n718)* allele lowers, rather than elevates, the abundance of

237   mtDNA^{uaDf5} (mtDNA^{uaDf5}:mtDNA^{WT} molar ratio of 1.8:1, Fig. 2C). This effect is likely to be

238   attributable to the nature of the *n718* mutation. Those *ced-3* mutations that result in increased

239   mtDNA^{uaDf5} levels (Fig. 2A) both alter the p15 domain, which is essential to the active caspase

240   function. In contrast, the *n718* mutation changes a residue in the caspase activation and

241   recruitment domain (CARD), located within the prodomain of the CED-3 zymogen, which is

242   removed upon caspase activation and affects its activation by CED-4 (Fig. 2 – figure supplement

243   3) [44,54]. While *ced-3(n718)* strongly compromises PCD, this mutation might not alter CED-3

244   caspase function in a way that interferes with its role in mtDNA purifying selection.

245   Our surprising finding that while CED-3 activity is required for mtDNA purifying selection,

246   a CED-3 mutation that compromises its activation by CED-4 did not elevate mtDNA^{uaDf5} levels

247   prompted us to investigate the requirement of CED-4 in mitochondrial purifying selection.

248   Consistent with the effect of the *ced-3(n718)* mutation, we found that eliminating the function

249   of the pro-apoptotic regulator CED-4, the *C. elegans* orthologue of mammalian Apaf1 and the

250   upstream activator of CED-3 in the canonical PCD pathway [60,69], did not result in a marked

251   increase in the relative abundance of mtDNA^{uaDf5}. That is, while the mtDNA^{uaDf5}:mtDNA^{WT} molar

252   ratio increased to 3.1:1 in the *ced-4(n1894)* mutant, the effect was not statistically significant.

253   Moreover, the canonical allele *ced-4(n1162)* allele similarly showed no elevation in mtDNA^{uaDf5}

254   (molar ratio = 2.6:1; Fig. 2B). These results suggest that CED-3 caspase functions in mitochondrial

255   purifying selection independently of the caspase-activating factor CED-4.

256

257   **Evidence that decreased fitness, but not lifespan, is attributable to mtDNA^{uaDf5}-induced PCD**

258   Taken together, our results implicate many PCD regulatory factors, and potentially PCD, in

259   the selective clearance of defective germline mtDNAs. Our additional observations suggest that

260   defective mtDNAs may, in fact, *trigger* elevated germline PCD, resulting in the production of

261   fewer mature gametes and progeny. Specifically, we found that the significant decrease in brood

262   size that we observed in *uaDf5*-bearing animals with a wildtype nuclear background is partially

263   suppressed by both *ced-3(-)* and *ced-13(-)* mutations, which prevent PCD (Fig. 2D, Fig. 2 – figure

264   supplement 4A), suggesting that elimination of PCD might rescue cells that would otherwise be

265   provoked to die as a result of accumulation of defective mtDNA. Our findings further underscore

266   the observation that accumulation of defective mtDNA in those animals that do survive does not

267   affect longevity, as we found that lifespan is unaltered in these PCD mutants even when the levels

268   of mtDNA^{uaDf5} are nearly doubled (Fig. 2 – figure supplement 4B, C).

269

270   **Age-dependent accumulation of mtDNA^{uaDf5} in the germline**

271   Our findings that PCD regulators are required to reduce mtDNA^{uaDf5} abundance, the

272   central role that mitochondria play in PCD [31–33,70], the observed decline of mitochondrial

273   health during the aging process [7,35–37,71–75], and the relationship between excessive PCD

274   and the aging phenotype [34] led us to examine the dynamics of mtDNA^{uaDf5} accumulation as

275   worms age. We measured the fractional abundance of *uaDf5* in adults at progressively increased

276   ages spanning day 1, defined as the first day of egg-laying, through day 10. Day 1 through day 4

277   of adulthood encompasses the time during which nearly all self-progeny are produced. After day

278   4, hermaphrodite sperm become depleted and the animals transition into a post-gravid,

279   progressively aging state [76–78]. By day 10, animals exhibit indications of advanced age. Analysis

280   of the abundance of mtDNA^{uaDf5} revealed a progressive increase throughout gravidity and post-

281   reproductive aging, with the mtDNA^{uaDf5}:mtDNA^{WT} molar ratio increasing from 2.9:1 to 5.5:1 (Fig.

282   3A, Fig. 3 – figure supplement 1A). This age-related accumulation of *uaDf5* in adult worms is

283   reminiscent of the accumulation of mtDNA mutations seen in aging mammals [35,73,79] and

284   suggests that *uaDf5* in *C. elegans* may be a useful tool for studying the role that mtDNA mutations

285   play in aging.

286   Given that gametes are depleted with age, it is conceivable that the age-dependent

287   increase in mtDNA^{uaDf5} is attributable to accumulation in somatic mitochondria. To assess

288   whether the observed age-related accumulation of mtDNA^{uaDf5} occurs predominantly in the

289   maternal germline or in somatic cells, we analyzed animals defective in germline development

290   by taking advantage of the *glp-4(bn2)* mutant, which produces only a small number (~12) of

291   germline cells compared to that in wildtype animals (~1,500), with no known effect on somatic

292   gonad development [80]. In contrast to the increased mtDNA^{uaDf5} abundance with age seen at

293   permissive temperature (mtDNA^{uaDf5}:mtDNA^{WT} of 1.8:1 at day 1, rising to 2.6:1 at day 4, for an

294   overall increase by 48%), we found that *glp-4(bn2)* animals at the non-permissive temperature

295   showed a slight decrease in the defective mtDNA from day 1 to day 4 of adulthood (2.2:1 at day

296   1, dropping to 2:1 at day 4, for an overall decrease of 6.3%) (Fig. 3B). These results strongly

297   suggest that the observed age-dependent increase in mtDNA^{uaDf5} abundance occurs exclusively

298   in the germline. We found that mtDNA^{uaDf5} does eventually appear to accumulate in somatic cells

299   with age, as day 10 adults grown at the restrictive temperature showed a marked increase in the

300   mtDNA^{uaDf5}:mtDNA^{WT} molar ratio compared to day 1 adults even in the absence of a germline

301   (day 10 *glp-4(bn2)* molar ratio of 3.4:1, a 57% increase from day 1 levels) (Fig. 3B). We conclude

302   that the marked increase in mtDNA^{uaDf5} with age during the period of fecundity occurs primarily

303   in the germline and that the defective mtDNA accumulates in both germline and somatic tissue

304   during post-reproductive life.

305

Age-dependent increase in mtDNA^{uaDf5} burden is transmitted to progeny

306

307   As the mtDNA is inherited strictly through the maternal germline, we posited that the

308 age-dependent increase in the fractional abundance of germline mtDNA^{uaDf5} might be

309 transmitted to progeny animals. To test this hypothesis, we measured the molar ratio of

310 mtDNA^{uaDf5} in 200-worm populations of L1 larvae derived from day 1 – day 4 adults (Fig. 3C, Fig.

311 3 – figure supplement 1B). This analysis led to two key observations: 1) the abundance of

312 mtDNA^{uaDf5} is reduced during transmission between mother and offspring (average decrease

313 ranging from 6% to 13%), presumably as a result of purifying selection, and 2) the abundance of

314 the defective mtDNA in the offspring correlates with the age of the mothers: the progeny of older

315 mothers contain a markedly higher mtDNA^{uaDf5}:mtDNA^{WT} molar ratio (4.2:1) than that of younger

316 mothers (2.6:1) (Fig. 3C, D). A similar trend was observed for mother-to-offspring transmission in

317 five mutant strains with altered levels of mtDNA^{uaDf5} (see below): in all cases, progeny contain

318 lower abundance of mtDNA^{uaDf5} than their mothers, and progeny of younger adults inherit a

319 lower load of mtDNA^{uaDf5} than progeny of older adults (Fig. 3C). These results reveal that mtDNA

320 quality control occurs between primordial germ cell proliferation in the female germline and L1

321 hatching, i.e., during oocyte maturation, embryogenesis, or both.

322

The lifespan-determining IIS pathway regulates accumulation of mtDNA^{uaDf5}

323

324   We sought to determine whether the age-dependent accumulation of defective mtDNA

325 is controlled by known molecular mechanisms that drive the aging program in *C. elegans*. The

326 most prominent of these regulatory systems is the highly conserved insulin/IGF-1 (insulin-like

16

327   growth factor-1) pathway (IIS), which performs a pivotal regulatory function in aging and

328   longevity [28,82,83] (Fig. 4 – figure supplement 1). Abrogation of the IIS signaling pathways, for

329   example, as a result of mutations in the gene encoding the IIS receptor (DAF-2, in *C. elegans*),

330   results in marked slowing of the aging program and extension of lifespan in worms, flies, and

331   mice [84–87]. The IIS pathway also functions in a broad set of other processes including, in *C.*

332   *elegans*, activation of two stages of developmental arrest, or diapause, at the L1 larval stage and

333   in formation of the dispersal form, the dauer larva, as well as in the control of germline

334   proliferation, stress resistance, fat metabolism, and neuronal/behavioral programs [28]. It was

335   also reported that inhibition of the IIS pathway rescues various fitness parameters in a mtDNA

336   mutator strain which contains a faulty mtDNA polymerase [29], consistent with a possible role in

337   mtDNA quality control.

338   We found that two mutant alleles of *daf-2*, which reduce rates of aging and increase

339   lifespan, result in dramatically decreased mtDNA^{uaDf5}:mtDNA^{WT} molar ratios from 2.8:1 to as low

340   as 0.3:1 (0.3:1 for *daf-2(e1391)*; 0.8:1 for *daf-2(e1370)*; Fig. 4A; see Suppl. Table 2 for a list of

341   lifespan mutants used in the analyses). Thus, the lifespan-extending effects of *daf-2* mutations

342   are strongly correlated with diminished abundance of defective mtDNA, to the extent that it

343   becomes the minor species of mtDNA.

344   The DAF-2 receptor acts by antagonizing the DAF-16/FoxO transcription factor, the major

345   effector of IIS downstream, in response to insulin-like ligands. Thus, removal of *daf-16* function

346   reverses the lifespan-extending effects of *daf-2(-)* mutants. We tested whether the DAF-2 → DAF-

347   16 pathway similarly functions in mtDNA purifying selection. We found that eliminating DAF-16

348   in two *daf-16* mutants results in slightly increased, albeit not statistically significant,

17

349 mtDNA^{uaDf5}:mtDNA^{WT} molar ratios (3.3:1 for *daf-16(mu86)*; 3.5:1 for *daf-16(mgDf50)*) (Fig. 4B).

350 Further, we found that removal of DAF-16 in the *daf-16(mu86)* mutant suppressed the decreased

351 mtDNA^{uaDf5}:mtDNA^{WT} molar ratios observed in two *daf-2* mutants, from 0.3:1 for *daf-2(e1391)* to

352 1:1 for *daf-16(mu86); daf-2(e1391)* and from 0.6:1 for *daf-2(e1370)* to 1.8:1 for *daf-16(mu86);*

353 *daf-2(e1370)*, consistent with observations reported in a recent study [88]. While the *daf-2(-)*

354 effect on mtDNA^{uaDf5} levels is largely dependent on DAF-16, neither double mutant restored

355 mtDNA^{uaDf5} levels to those seen in animals with a fully intact IIS pathway, suggesting that other

356 DAF-2 targets might participate in removal of defective mtDNA (Fig. 4C). We found, conversely,

357 that two mutations that reduce lifespan by eliminating the function of AAK-2 (AMP activated

358 kinase-2), a conserved factor acting in the IIS pathway [28,89], result in elevated

359 mtDNA^{uaDf5}:mtDNA^{WT} molar ratios as high as 4.4:1 compared to 2.8:1 in wildtype animals (3.8:1

360 for *aak-2(ok524)* and 4.4:1 for *aak-2(gt33)*) (Fig. 4B). These findings demonstrate that alterations

361 in the IIS pathway coordinately affect both lifespan and accumulation of defective mtDNA and

362 that the DAF-2/DAF-16/AAK-2 axis acts similarly in both processes.

363

364 **Synergistic effect of multiple aging pathways on mtDNA^{uaDf5} accumulation**

365 In addition to IIS, other molecular regulatory pathways independently contribute to the

366 rate of aging. These include CLK-1, a mitochondrial hydroxylase that functions in the pathway for

367 ubiquinone synthesis [90,91]. *clk-1* mutants with a wildtype mitochondrial genome have been

368 shown to contain levels of mtDNA that are elevated by 30%, perhaps as the result of a

369 compensatory process that increases demand on mitochondrial abundance, or the action of CLK-

370 1 as a regulator of mtDNA abundance in response to energy availability within the cell [92]. As

18

371   with long-lived *daf-2* mutants, we found that long-lived *clk-1(qm30)* mutants showed a greatly

372   diminished mtDNA^{uaDf5}:mtDNA^{WT} molar ratio of 0.3:1 (Fig. 4A), comparable to that in *daf-2*

373   mutants; again, mtDNA^{uaDf5} is the minor species in these animals. As the IIS pathway and CLK-1

374   appear to act separately in controlling lifespan, we postulated that elimination of both

375   mechanisms might further reduce levels of the defective mtDNA. Indeed, we found that

376   mtDNA^{uaDf5} was completely eliminated in *daf-2(e1391) clk-1(qm30)* double mutants, revealing a

377   strongly synergistic effect between the two age-determining systems (Fig. 4A). Thus, distinct

378   regulatory pathways for longevity modulate the abundance of mtDNA^{uaDf5} by apparently different

379   mechanisms and elimination of the two pathways abrogates its maintenance.

380

381   **Age-dependent accumulation rate of mtDNA^{uaDf5} strongly correlates with genetically altered**

382   **rates of aging**

383   Our findings that the steady-state abundance of mtDNA^{uaDf5} increases with maternal age

384   and that mutants with increased lifespan show lower levels of the defective mtDNA raised the

385   possibility that purifying selection is subject to the same control as aging clocks. To assess this

386   potential connection, we analyzed the time-dependent rates of mtDNA^{uaDf5} accumulation in

387   animals with genetic backgrounds that alter the aging clock. Analysis of 21 different genetic

388   backgrounds over the first ten days of adulthood revealed that the age-dependent progressive

389   accumulation of mtDNA^{uaDf5} is a consistent phenomenon (Fig. 4D). Comparison of long-lived

390   mutants and wildtype using a linear regression model revealed a striking positive correlation

391   between aging rate and age-dependent rate of accumulation of mtDNA^{uaDf5}: all long-lived

392   mutants in either the IIS pathway or *clk-1* accumulate mtDNA^{uaDf5} at a substantially slower rate

393   as they age than do wildtype animals (Fig. 4E, Fig. 4 – figure supplement 2A, B). Conversely, we

394   analyzed six short-lived IIS pathway mutant combinations and found that the *aak-2(ok524)* and

395   *daf-16(mu86)* single mutants and *daf-16(-);daf-2(-)* double mutants all showed increased rates of

396   mtDNA^{uaDf5} accumulation (Fig. 4E, Fig. 4 – figure supplement 2C, D). These observations suggest

397   that in both slower-aging and faster-aging strains, the rate of accumulation of deleterious mtDNA

398   is a predictor of aging rate. In the two exceptional cases, the *aak-2(gt33)* and *daf-16(mgDf50)*

399   single mutants, we did not observe an increased accumulation rate compared to wildtype;

400   however, the mtDNA^{uaDf5} levels are consistently higher than in these two mutants than in

401   wildtype at all stages (Fig. 4E, Fig. 4 – figure supplement 2D) and thus diminished removal of

402   mtDNA^{uaDf5} overall correlates with decreased lifespan in these mutants as well. The greater

403   mtDNA^{uaDf5} accumulation rates seen in the short-lived animals is not attributable to the higher

404   steady-state levels *per se*, as the rates of accumulation of defective mtDNA observed in the PCD

405   mutants with higher mtDNA^{uaDf5} levels show no correlation with the steady-state levels (Fig. 4 –

406   figure supplement 2 E-H); rather these increased rates appear specifically to be a property of the

407   shortened lifespan mutants.

408   Consistent with a relationship between aging rates and accumulation of defective mtDNA,

409   we found that brood size is decreased and embryonic lethality is increased in short-lived *daf-16(-*

410   *)* mutants compared to those in a wildtype nuclear background, while *uaDf5* does not impact

411   either fitness parameter in the long-lived *clk-1* mutant (Fig. 4 – figure supplement 3). These

412   results are consistent with the possibility that longevity pathways modulate fitness in part by

413   regulating mitochondrial homeostasis.

414

415   **Evidence for late adulthood-specific mechanisms for removal of mtDNA^{uaDf5}**

416   We obtained evidence that defective mtDNA is more effectively removed in offspring of

417   aging adults that carry an unusually high burden of mtDNA^{uaDf5}. The offspring of day 4 adults in

418   those strains ("high" strains) with significantly higher steady-state fractional abundance of

419   mtDNA^{uaDf5} showed significantly greater rates of reduction of the defective mtDNA (reduction

420   from 5.4:1 to 3.3:1 in *atfs-1(et15)*, from an extraordinarily high 6.5:1 to 2.8:1 in *ced-10(n1993),*

421   and from 6.4:1 to 3.3:1 in *ced-13(sv32)*) compared to offspring of ("low" strain) mothers with

422   lower steady-state fractional abundance of the mutant mtDNA (reduction from 4.7:1 to 4.2:1 in

423   WT, from 3.9:1 to 2.8:1 in *ced-3(n2454),* and from 3.2:1 to 2.5:1 in *ced-4(n1162)*). Remarkably,

424   therefore, day 4 progeny from "high" strains actually inherit a *lower* mtDNA^{uaDf5} load than their

425   siblings born from day 1-3 mothers (Fig. 3C, 5A). Indeed, we found a strong correlation (r^2=0.61,

426    $p < 0.001$) between the steady-state level of mtDNA^{uaDf5} in mothers and the capacity for its

427   removal between mother and progeny during day 4 of adulthood (Fig. 5B). These results raise

428   the possibility that very high levels of mtDNA^{uaDf5} in older mothers activate additional mtDNA

429   purifying selection independent of the UPR^{MT} and PCD machinery, thereby ensuring that progeny

430   are not overloaded with defective mitochondria.

431

Discussion

432

433   We have obtained several lines of evidence indicating that regulators of PCD and the aging

434   program function in mtDNA quality control and accumulation of defective mtDNA in *C. elegans*.

435   We report eight major findings: 1) regulators of germline PCD are required for effective removal

436   of deleterious mtDNA from the germline; 2) the cell death machinery functions in either a non-

437   canonical cell death pathway or in a non-apoptotic role to mediate mitochondrial purifying

438   selection; 3) the CSP-1 caspase has as strong of an effect on mitochondrial purifying selection as

439   the major PCD regulator CED-3; 4) mtDNA^{uaDf5} progressively accumulates in the germline as

440   adults age; 5) this age-dependent accumulation of mtDNA^{uaDf5} is transmitted to progeny;

441   however, the burden of the defective mtDNA is lower in offspring than mothers suggesting

442   intergenerational purifying selection; 6) two separate aging pathways, the IIS and CLK-1

443   pathways, act synergistically to regulate mtDNA^{uaDf5} levels; longer-lived mutants show reduced

444   levels of the defective mtDNA while shorter-lived mutants show increased levels compared to

445   otherwise wildtype animals; 7) the rate of mtDNA^{uaDf5} accumulation is inversely correlated with

446   lifespan in aging mutants; 8) intergenerational removal of mtDNA^{uaDf5} occurs more effectively

447   during transmission from older mothers with high burden of the defective mtDNA.

448   Previous reports demonstrated that UPR^{MT} limits *uaDf5* clearance, and that eliminating

449   the UPR^{MT}-mediating transcription factor, ATFS-1, lowers mtDNA^{uaDf5} abundance [25,27]. Our

450   identification of a second mutation in the *uaDf5* mutant that results in premature truncation of

451   the ND4 gene product raises the possibility that expression of both the truncated ND4 and the

452   ND1-CYTB fusion protein might together activate UPR^{MT}. The possibility that it is the production

453   of aberrant polypeptides resulting from these mutations that trigger this response will require

454   analysis of additional mtDNA mutants.

455

456   **Mitochondrial deletion mutant *uaDf5* as a model for mitochondrial disease**

457   We found that *uaDf5* affects brood size, embryonic lethality, and developmental rate,

458   highlighting its use as a model for investigating mitochondrial diseases. The reduced brood size

459   in *uaDf5*-bearing animals might reflect diminished germ cell proliferation, as mitochondria have

460   been implicated in progression of germline maturation [93,94]. Alternatively, the defective

461   mtDNA might trigger hyperactivation of the germline PCD pathway that specifically removes

462   germ cells with the highest burden of defective mtDNA, as suggested by our results, resulting in

463   the survival of fewer mature oocytes. The increased embryonic lethality in the *uaDf5* strain may

464   be a consequence of a genetic bottleneck effect, leading to rapid differences in mtDNA allele

465   frequencies [95–97] and a subpopulation of oocytes containing levels of mtDNA^{uaDf5} that exceed

466   a threshold required for viability.

467   We were surprised to find, in contrast to a previous report [98], that mtDNA^{uaDf5} did not

468   alter lifespan. Given that mitochondrial mutations are often coupled with compensatory

469   mutations in the nuclear genome [99–103], one possible explanation for this discrepancy might

470   be that a compensatory nuclear mutation exists in the strain analyzed, diminishing the impact of

471   the defective mitochondrial genome. We note, however, that we backcrossed the *uaDf5* strain

472   extensively to the laboratory reference strain N2 prior to performing the reported analyses. It is

473   conceivable that although we observed no effect in the lab, *uaDf5* might alter lifespan under

474   natural conditions. Exposure to increased stress from growth in the wild might be less tolerated

23

475   in animals bearing mtDNA^{uaDf5}, as has been observed with other mitochondrial mutants [104],

476   resulting in diminished lifespan.

477

478   **Caspases and cell death machinery regulate mitochondrial purifying selection**

479   Our results lend support to the hypothesis that germline PCD mechanisms may be used

480   to cull germline cells with defective mtDNA (Fig. 6A). Developmentally programmed cell death

481   and cell death in response to genotoxic stress are mediated by caspases upon activation by the

482   *C. elegans* octameric apoptosome which is formed when the inhibition of CED-4 by CED-9 is

483   disrupted through binding of BH-3-only proteins EGL-1 and CED-13 in the soma and germline,

484   respectively. We propose that in response to mitochondrial genotoxic stress (increased

485   mtDNA^{uaDf5} load), caspases CED-3 and CSP-1 are activated by the BH-3 only domain protein CED-

486   13 thereby triggering mitochondrial purifying selection independent of CED-9 and the CED-4

487   apoptosome, either through germ cell PCD or a non-apoptotic role of these caspases (Fig. 6A).

488   Mutations that eliminate the function of caspases that act in PCD result in elevated

489   mtDNA^{uaDf5} levels. Two mutations affecting the p15 domain of the CED-3 caspase result in a

490   significantly increased molar ratio of *uaDf5*, highlighting the importance of the p15 domain in

491   mtDNA quality control. It is noteworthy that the two mutations that result in a more substantial

492   effect on mtDNA^{uaDf5} abundance affect CED-3 structure more dramatically: *ced-3(n717)* results in

493   a splicing error, and *ced-3(n1286)* is a nonsense mutation [54]. In contrast, *ced-3(n2454)*, which

494   results in a subtle (statistically insignificant) increase in mtDNA^{uaDf5}, is a substitution predicted to

495   impart a much weaker effect on the protein structure [54]. The effect of the *ced-3(n718)* allele,

496   which resides in the prodomain of CED-3, suggests that that portion of the protein may act to

24

497   inhibit mtDNA quality control. Taken together, our results suggest that CED-3 may carry out a

498   specialized activity in mtDNA-activated PCD. We found that a second caspase, CSP-1, which plays

499   a minor role in PCD [56,57], is also required in mtDNA quality control: a *csp-1(-)* knockout

500   mutation results in increased abundance of mtDNA^{uaDf5} and enhances the effect of *ced-3(n717)*,

501   suggesting that CSP-1 may play a larger role in removal of defective mtDNA than it does in other

502   forms of PCD. An exciting possibility is that caspases act in mtDNA quality control via a mechanism

503   that is distinct from their normal action in PCD. Such putative roles for caspases and other

504   mitochondrial factors in non-apoptotic mitochondrial quality control may have been co-opted

505   during metazoan evolution with the innovation of PCD.

506   Analysis of additional PCD components further implicate a role for germline PCD in

507   mitochondrial purifying selection. These include CED-13, the germline-specific PCD effector, and

508   components of the cell corpse engulfment pathway, which activate PCD likely through a complex

509   feedback mechanism that ensures cells destined to die proceed irreversibly through the process

510   [66,67]. In all cases, mutations in these components result in increased mtDNA^{uaDf5} levels. In

511   vertebrates, mitochondrial reactive oxygen species (mtROS) trigger apoptosis via the intrinsic

512   mitochondrial pathway [120]. Interestingly, elevated mtROS promotes longevity that is in part

513   dependent on the core cell death machinery in *C. elegans*, involving CED-9, CED-4, CED-3 and

514   CED-13, but not EGL-1 [105]. In that study, the authors reported that the protective effect of the

515   cell death machinery on lifespan was independent of PCD in the soma; however, germline cell

516   death was not characterized. Given that CED-13, and not EGL-1, is the predominant BH3-domain

517   protein functioning in the germline [58] and that ablation of the germline leads to extended

518   lifespan [106], our findings support the possibility that germline progenitors carrying defective

25

519   mitochondria selectively undergo PCD, ensuring homeostatic mtDNA copy number and health of

520   progeny.

521   A striking exception to our findings was seen with mutations that eliminate the function

522   of the pro-apoptotic regulator CED-4. Neither the *ced-3(n718)* mutation that disrupts the CED-3

523   CARD domain, which is involved in recruitment to the apoptosome by stabilizing its interaction

524   with CED-4 [44,107], nor two *ced-4(-)* mutations, result in increased accumulation of mtDNA^{uaDf5},

525   suggesting non-canonical, CED-4-independent activation of CED-3 in mitochondrial purifying

526   selection. It is possible that the CARD mutation (G65R) in the *ced-3(n718)* mutant [54] reduces

527   the fraction of CED-3 in complex with the apoptosome, which might release more of the protein

528   for its role in mitochondrial purifying selection. Interestingly, the CARD linker domain has been

529   found to have an inhibitory effect on the pro-caspase-9 zymogen [108]. *ced-3(n718)* could be

530   effectively acting as a gain-of-function allele in the process of purifying selection, reflected by the

531   lower levels of mtDNA^{uaDf5} in this mutant background.

532   It is noteworthy that CED-4 and its mammalian Apaf1 relatives regulate a variety of

533   cellular functions that are unrelated to their activities in PCD. These include cell growth control

534   influenced by DNA damage, centrosomal function and morphology, neuronal regeneration, and

535   inhibition of viral replication [109–112]. In addition, as a result of differential RNA splicing, *ced-4*

536   encodes proteins with opposing activities, generating both an activator and a repressor of

537   apoptosis [113], which further complicates analysis of its action. Thus, it is conceivable that CED-

538   4 might exert opposing effects on purifying selection, reflecting its pleiotropic activities in

539   development and confounding an unambiguous interpretation of its action in this process.

540

26

541   **IIS and CLK-1 synergistically regulate germline accumulation of mtDNA^{uaDf5} as adults age**

542   We found that most of the increase in the fractional abundance of mtDNA^{uaDf5} as worms

543   age throughout the period of self-fertility (days 1-4) occurs in the germline. However, the relative

544   amount of the defective mtDNA continues to increase in older animals when the germline is no

545   longer actively proliferating [76], suggesting that mtDNA proliferation also occurs in somatic

546   tissues throughout the aging process. This behavior mirrors the dynamics of mutant mtDNAs

547   observed in other organisms, including human, mouse, rat, and rhesus monkey [35,73,79]. While

548   removal of the germline in worms results in extended lifespan [114,115], it is not clear whether,

549   or to what extent, this increased lifespan might be attributable to accumulation of mutant

550   mtDNA, since the lack of germline leads to a variety of cellular responses [116,117], any of which

551   might lead to lifespan extension.

552   These studies do not reveal whether, or how, aging and accumulation of defective mtDNA

553   are causally linked. However, our findings that steady-state levels of mtDNA^{uaDf5} are lowered in

554   long-lived mutants (*daf-2* (IIS pathway; [28]) and *clk-1* (mitochondrial function; [118,119])) and

555   that rates of its accumulation are strongly inversely correlated with lifespan extension through

556   independent pathways, suggests that mtDNA purifying selection mechanisms are influenced by

557   aging programs (Fig. 6A). Further bolstering this potential link is our finding that short-lived

558   mutants (*daf-16* and *aak-2,* both involved in the IIS pathway [28]), show higher steady-state levels

559   of mtDNA^{uaDf5}. That this effect is greater in *aak-2* mutants than in *daf-16* mutants suggests that

560   the AAK-2 branch of the IIS pathway influences mtDNA quality control more significantly than

561   does the DAF-16 branch. One of the substrates of AAK-2 is SKN-1/Nrf2, a multifaceted

562   transcription factor with roles in stress response and longevity, and one of its isoforms, SKN-1a,

27

563   localizes to the mitochondrial surface [120], raising the possibility that AAK-2 might influence

564   clearance of defective mtDNA through SKN-1 action. It will be of interest to assess how defective

565   mtDNA might coordinately trigger quality control and stress-response pathways.

566   Our observation that IIS pathway components and CLK-1 act synergistically on the mtDNA

567   quality control machinery raises the possibility that these two distinct lifespan-regulating

568   pathways converge on a common system for removal of defective mtDNA, such as a global

569   mitochondrial stress response pathway. Candidates for mediating this removal process include

570   mitochondrial fission/fusion [17,20,121], mitophagy [18,19,122], and the UPR[MT] [22–27], all of

571   which are known to act in mtDNA quality control, as well as modulation of the regulatory

572   pathway for PCD, as suggested by our findings.

573

574   **PCD is uncoupled from aging during intergenerational mitochondrial purifying selection in**

575   **older mothers**

576   Analysis of newly hatched L1 larvae revealed that the relative load of mtDNA^{uaDf5} is

577   transmitted from mother to offspring, with evidence for intergenerational purifying selection

578   (Fig. 6B). This finding implies that mtDNA quality control occurs between germline stem cell

579   expansion in the mature female germline and L1 hatching, a developmental period that spans

580   many potential stages at which it might occur, including germline PCD, oocyte maturation, and

581   the entirety of embryogenesis. It is conceivable that this selection process acts at multiple stages

582   throughout this developmental window and that the decreased burden of defective mtDNA in

583   newly hatched L1 larvae reflect the summation of a series of sequentially acting processes that

584   incrementally enrich for healthy mtDNA.

585   The efficacy of intergenerational removal of mtDNA^{uaDf5} increases in old mothers,

586   including in strains lacking pro-apoptotic regulators. The clearance is particularly precipitous in

587   strains with a very high burden of defective mtDNA as seen in the absence of CED-13, CED-10,

588   and ATFS-1, suggesting a critical threshold beyond which a germline PCD-independent mtDNA

589   quality control process may be triggered in these older mothers (Fig. 6B). One possible

590   explanation for this observation is that an mtDNA purifying selection mechanism that is typically

591   inhibited by germline PCD might be activated in older mothers. This hypothesized purifying

592   selection mechanism might be triggered by the unique cellular environment associated with

593   aging such as increased organelle or macromolecule damage. Alternatively, the effect might be

594   the result of an age-dependent genetic program.

595   While our study has uncovered new mechanisms acting in mtDNA purifying selection and

596   its relationship to aging, it is of note that some level of mtDNA^{uaDf5} is maintained in all but the

597   most extreme conditions we have observed (e.g., in the *daf-2(e1391) clk-1(qm30)* double

598   mutant, in which the defective mtDNA is extirpated). This finding raises the possibility that

599   some degree of heteroplasmy, even with defective mtDNA, is not only tolerated, but may be

600   adaptive by providing a degree of evolutionary plasticity. Cells might purposefully allow for

601   limited heteroplasmy as a way of increasing genetic heterogeneity that might prove

602   evolutionarily advantageous. Such heterogeneity may also be essential to allow mtDNA to co-

603   evolve with changes arising in the nuclear genome. It may be that a dynamic balance between

604   active mtDNA purifying selection, including the mechanisms identified here, and the

605   permissibility of limited heteroplasmy, is modulated according to environmental or

606   physiological demands.

29

607   **Materials and Methods**

608

609   **Culturing of nematodes**

610   Nematode strains were maintained on NGM plates as previously described at either 20°C

611   or 15°C for the temperature-sensitive strains [123]. Supplementary Tables 1, 2 and 3 provide

612   details of all strains used in this study. Strains without a JR designation were either provided by

613   the CGC which is funded by NIH Office of Research Infrastructure Programs (P40 OD010440) or

614   were obtained from the Mitani lab (strains with a FX designation or JR strains containing alleles

615   with a tm designation were generated from Mitani lab strains) [124].

616   **Population collection by age**

617   Upon retrieval of a stock plate for a given strain, three chunks were taken from the stock

618   plate and placed onto three separate large NGM plates to create three biological replicates

619   ("lines"). Each of these lines was chunked approximately each generation to fresh large NGM

620   plates (every 3 days if maintained at 20°C or 25°C, or every four days if maintained at 15°C, being

621   careful to not let the worms starve between chunks). After four generations of chunks, an egg

622   prep was performed on each line (as described previously; [123]) and left to spin in M9 overnight

623   to synchronize the hatched L1s. The next day, each egg prep was plated onto three large seeded

624   plates at an equal density and the worms were left to grow to day 2 adults (second day of egg

625   laying). The day 2 adult worms were egg prepped for synchronization and left to spin in M9 buffer

626   overnight. The next day, each egg prep was plated onto five large NGM plates at equal density.

627   Once the worms reached day 1 of adulthood (first day of egg-laying), one of the plates was used

628   to collect 200 adult worms by picking into 400 µl of lysis buffer, and the remaining adults on the

629   plate were egg prepped for the collection of hatched L1 larvae in 400 µl lysis buffer the following

30

630   day. The worms on the four remaining plates were transferred to a 40 μm nylon mesh filter in

631   order to separate the adults from the progeny, and the resulting adults were resuspended in M9

632   and pipetted onto fresh large NGM plates. This process was repeated for the following three days

633   (Day 2-4 of adulthood). Day 5-10 adults were moved to fresh NGM plates every 2nd day using a

634   40 μm nylon mesh filter, and the resulting day 10 adults were collected in lysis buffer.

635   **ddPCR**

636   The worm lysates were incubated at 65°C for 4 hours and then 95°C for 30 minutes to

637   deactivate the proteinase K. Each lysate was diluted; 100-fold for 200 worm adult population

638   lyses, 2-fold for 200 worm L1 population lyses, and 25-fold for individual adult lyses. 2 μl of the

639   diluted lysate was then added to 23 μl of the ddPCR reaction mixture, which contained a

640   primer/probe mixture and the ddPCR probe supermix with no dUTP. The primers used were:

641   WTF: 5'-GAGGGCCAACTATTGTTAC-3'

642   WTR: 5'-TGGAACAATATGAACTGGC-3'

643   UADF5F: 5'-CAACTTTAATTAGCGGTATCG-3'

644   UADF5R: 5'-TTCTACAGTGCATTGACCTA-3'

645   The probes used were:

646   WT: 5'-HEX-TTGCCGTGAGCTATTCTAGTTATTG-Iowa Black® FQ-3'

647   UADF5: 5'-FAM-CCATCCGTGCTAGAAGACAAAG- Iowa Black® FQ-3'

648   The ddPCR reactions were put on the BioRad droplet generator and the resulting droplet-

649   containing ddPCR mixtures were run on a BioRad thermocycler with the following cycle

650   parameters, with a ramp rate of 2°C/sec for each step:

651   1. 95°C for 5 minutes

31

652   2. 95°C for 30 seconds

653   3. 60°C for 2 minutes

654   4. Repeat steps 2 and 3 40x

655   5. 4°C for 5 minutes

656   6. 90°C for 5 minutes

657 After thermocycling, the ddPCR reaction plate was transferred to the BioRad droplet reader and

658 the Quantasoft software was used to calculate the concentration of mtDNA^{uaDf5} (FAM positive

659 droplets) and mtDNA^{WT} (HEX positive droplets) in each well.

660 **Lifespan analysis**

661   Confluent large plates were egg prepped and left to spin in M9 overnight for

662 synchronization. The hatched L1s were plated onto large thick plates and allowed to grow to day

663 2 adults before being egg prepped a second time and left to spin in M9 overnight. The next

664 morning, referred to as day 1 for lifespan determination, L1s were singled out onto small plates.

665 Once the worms started laying eggs, they were transferred each day to a fresh small plate until

666 egg laying ceased, after which the worms remained on the same plate unless bacterial

667 contamination required transfer to a fresh plate. Worms were considered dead if there was no

668 movement after being lightly prodded with a worm pick. Worms that died due to desiccation on

669 the side of the plate were excluded from analysis.

670 **Brood size and embryonic lethality analysis**

671   Confluent large plates were egg prepped and left to spin in M9 overnight for

672 synchronization. The hatched L1s were plated onto large thick plates and allowed to grow to day

673 2 adults before being egg prepped a second time and left to spin in M9 overnight. The next

674   morning, L1s were singled out onto small plates. Once the worms started laying eggs, they were

675   transferred each day to a fresh small plate until egg laying ceased. The day after transfer to a

676   fresh plate, unhatched embryos and hatched larvae on the plate from the previous day were

677   counted. This was done for each of the days of laying and the total of unhatched embryos and

678   hatched larvae from all plates from a single worm were tabulated to determine total brood size.

679   To determine embryonic lethality, the total number of unhatched embryos was divided by the

680   total brood size. Worms that died due to desiccation on the side of the plate were excluded from

681   analysis.

682   **Developmental time course analysis**

683   Confluent large plates were egg prepped and left to spin in M9 overnight for

684   synchronization. The hatched L1s were plated onto large thick plates and allowed to grow to day

685   2 adults before being egg prepped a second time and left to spin in M9 overnight. The next

686   morning, L1s were singled out onto small plates. The stage of the worms was assayed every 12

687   hours for the first 72 hours after plating. For determining the stage at 60 hours, L4 worms were

688   divided up into three subgroups based on morphology: young-L4, mid-L4, and late-L4; otherwise,

689   all other staged worms were not divided up into subgroups. Worms that died due to desiccation

690   on the side of the plate were excluded from analysis.

691   **Genotyping the *w47* allele**

692   DNA was collected from reference strain (N2) and two *uaDf5*-containing strains, LB138

693   and JR3630. Mitochondrial DNA was extracted and the DNA libraries were prepared using

694   Nextera Kit and then sequenced using an Illumina NextSeq500. Prior to alignment, reads from

695   fastq files were trimmed using Trimmomatic. Trimmed, pair-end reads (2x150) were then

696   mapped to the *C. elegans* assembly reference sequence WBcel235 using Burrows-Wheeler

697   Aligner (BWA) [125]. Picard Tools (http://broadinstitute.github.io/picard/) was used to mark

698   duplicate reads, and SAMtools [126] was used to merge, index and create pile-up format. VarScan

699   [127] was used to call variants, and only variants with minimum coverage of 100 and a minimum

700   variant frequency call of 0.01 were considered for analysis.

701   **Statistical Analysis**

702   Summary statistics, ANOVA, Mann-Whitney tests, and linear regression were calculated

703   using R v3.4.1. The details of the statistical tests are reported in the figure legends.

704

705 **Figures**

706 **Figure 1**
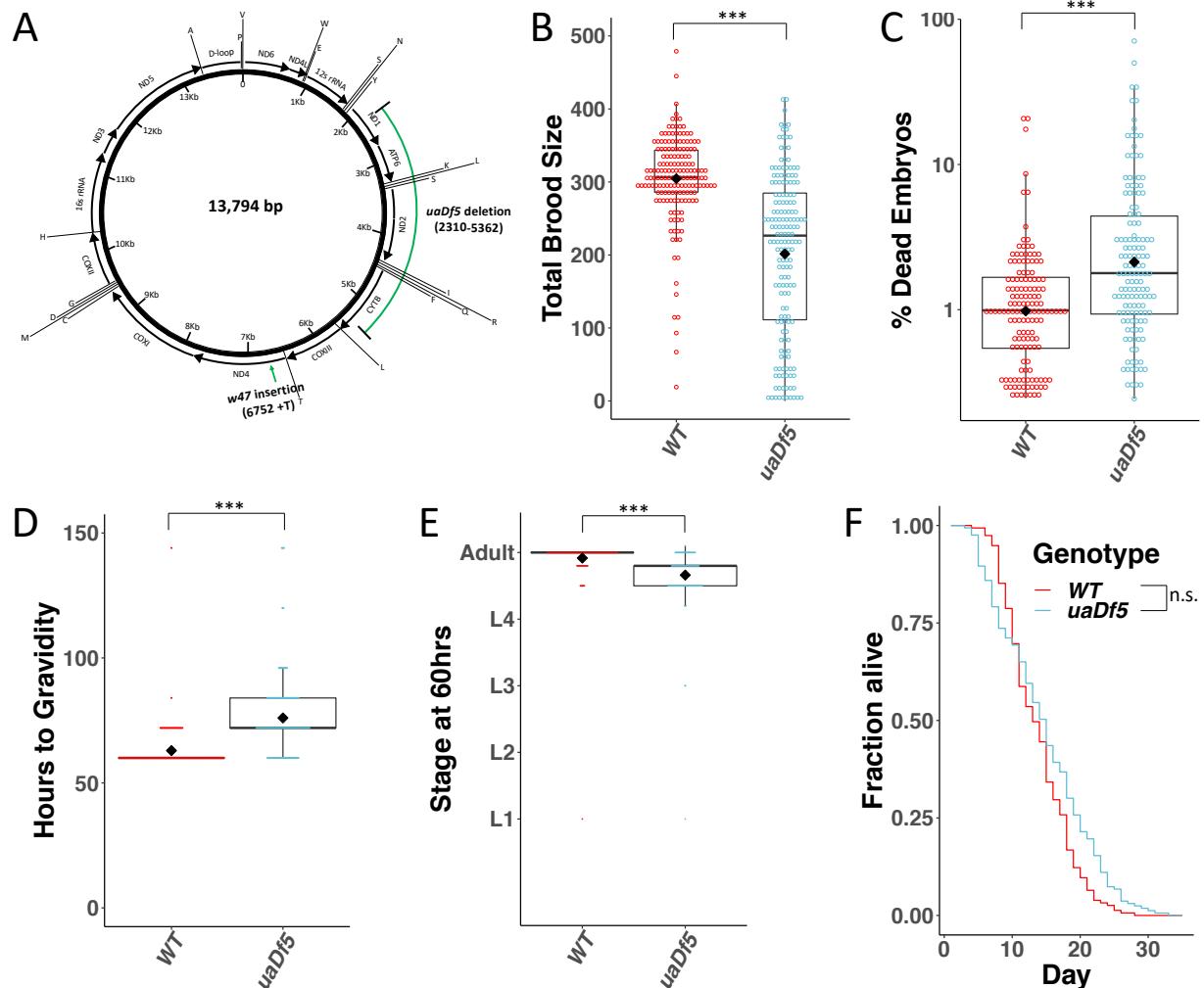
707
708 **Figure 1: Analysis of the impact of mtDNA^{uaDf5} on fitness parameters. (A)** Diagram of *C. elegans*

709 mtDNA. Black bars with arrows indicate the locations of genes and direction of transcription.

710 Black lines with letters indicate the locations of tRNAs. Green bars show the locations of the

711 mtDNA^{uaDf5} deletion as well as the linked *w47* insertion that was identified via Illumina

712 sequencing. **(B)** Brood size analysis of mtDNA^{uaDf5} compared to laboratory wildtype N2. **(C)**

713 Embryonic lethality analysis of *uaDf5* compared to laboratory wildtype N2. **(D)** Developmental

714 rate analysis of mtDNA^{uaDf5} compared to laboratory wildtype N2, counting how many hours it

35

715   takes for starved L1s to reach gravidity once plated on food. **(E)** Developmental rate analysis of

716   mtDNA^{uaDf5} compared to laboratory wildtype N2, staging worms 60 hours after synchronized,

717   staved L1s are plated on food. **(F)** Survival curve analysis of mtDNA^{uaDf5} compared to laboratory

718   wildtype N2, day 1 is defined as the day starved L1s are plated on food. Median lifespan and

719   statistics are presented in Supplemental Figure 2. For **B-E**, box plots show median and IQR, and

720   the diamond indicates the mean. Statistical analysis was performed using the Mann-Whitney

721   test. (*** $p < 0.001$, n.s. not significant).

722

723   **Figure 2**

724
725
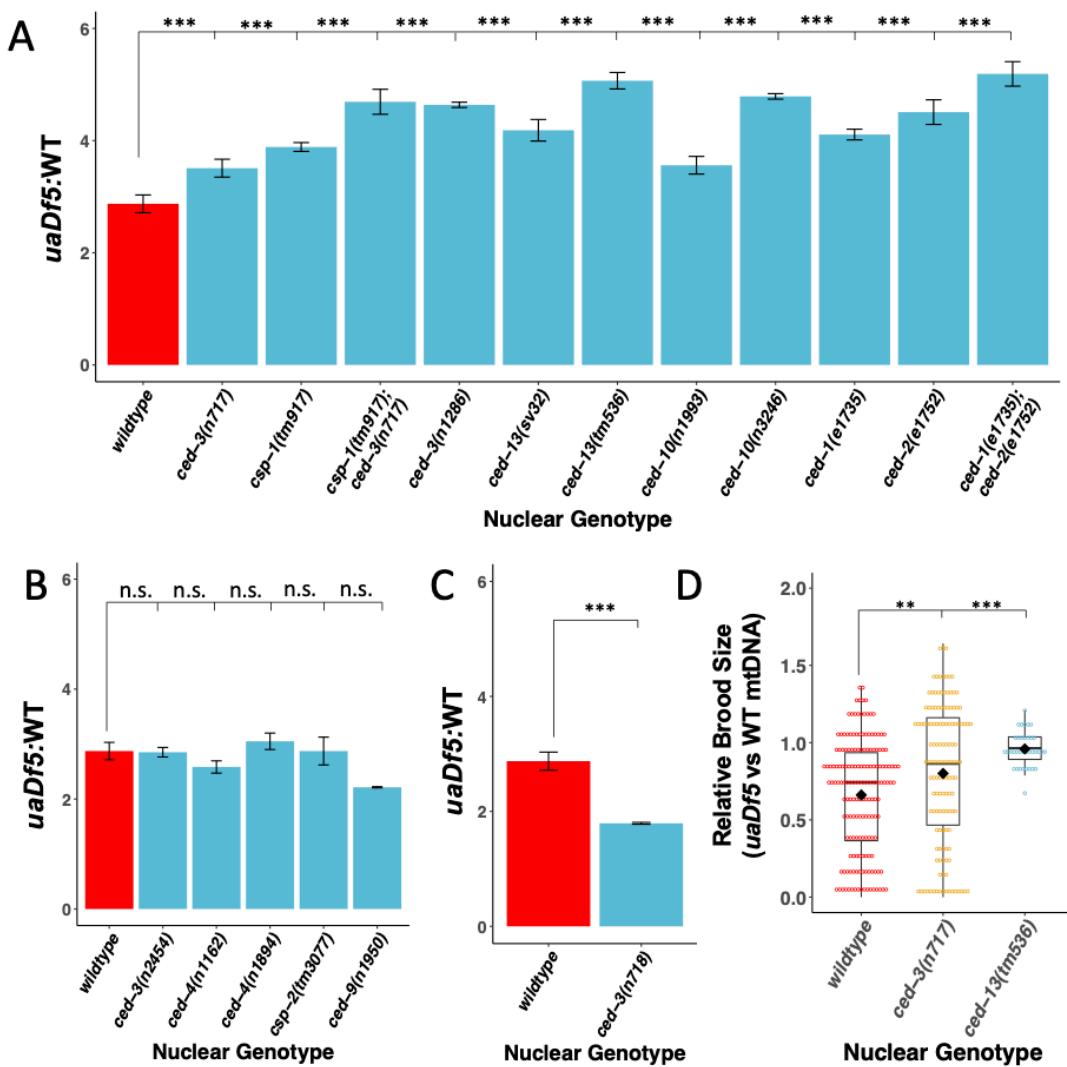
Figure 2: Regulators of PCD act on mutant mtDNA. (A-C) ddPCR analysis of the steady-state molar ratio of mtDNA^{uaDf5} in 200 worm populations of day 1 adults of various PCD mutant backgrounds. **(A)** PCD mutants that result in a significant increase in the molar ratio of mtDNA^{uaDf5}. **(B)** PCD mutants that result in no statistical change in the molar ratio of mtDNA^{uaDf5}. **(C)** PCD mutant that results in a significant decrease in the molar ratio of mtDNA^{uaDf5}. **(D)** The relative brood size of the animals with and without mtDNA^{uaDf5} in the indicated mutant backgrounds. For each nuclear genotype shown, the brood size of *uaDf5*-containing worms was

37

733   normalized by dividing by the average brood size of worms containing only *WT-mtDNA*. Box plots

734   show the median and IQR, the diamond indicates the mean. For **A-C**, n=3 or more biological

735   replicates of 200 worm populations were performed for each genotype. Statistical analysis was

736   performed using one-way ANOVA with Dunnett's correction for multiple comparisons. For **D**,

737   statistical analysis was performed using the Mann-Whitney test. Error bars represent SEM. (***

738    $p < 0.001$, ** $p < 0.01$, * $p < 0.05$, . $p < 0.1$, n.s. not significant).

739

740 **Figure 3**
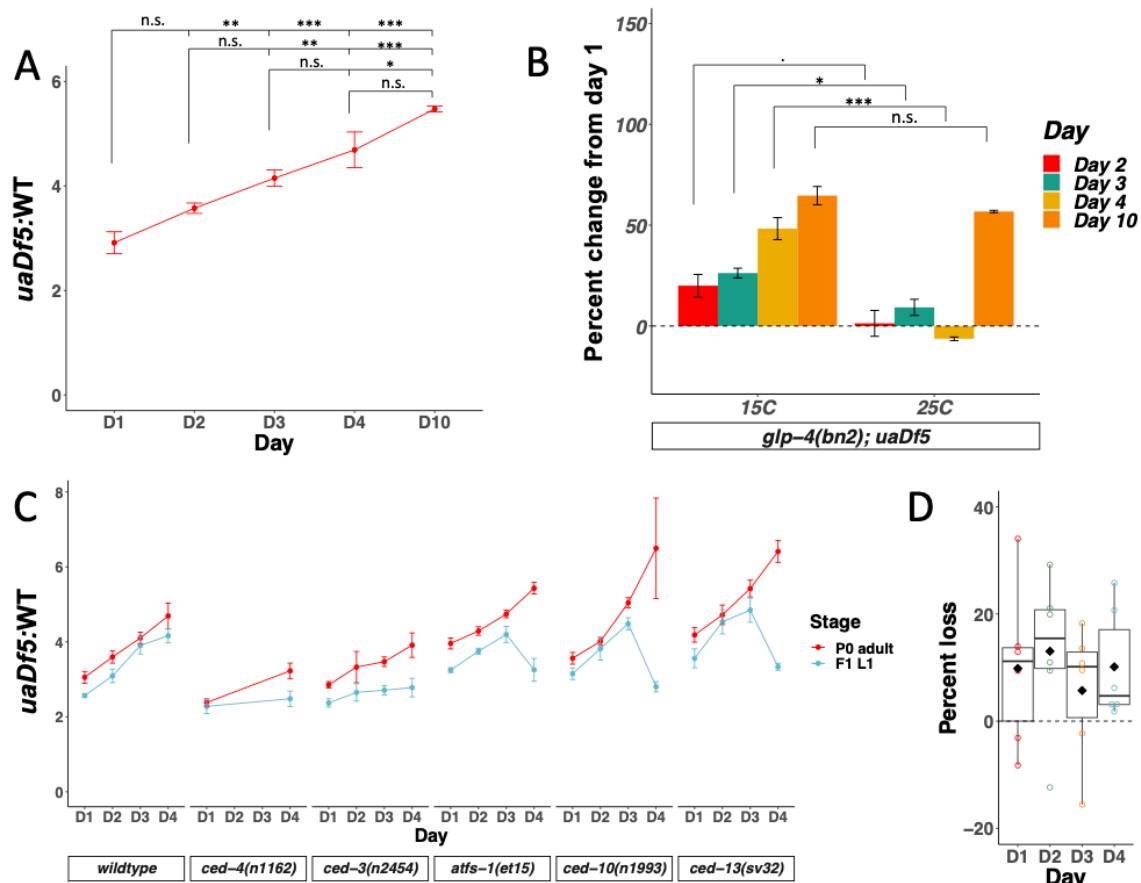
741

742 **Figure 3: mtDNA^{uaDf5} accumulates in the germline of aging adults, and evidence of purifying**

743 **selection between mother and offspring. (A)** Analysis of the molar ratio of mtDNA^{uaDf5} in aging

744 adults in a wildtype nuclear background. **(B)** Analysis of the percent change of *uaDf5:*WT from

745 day 1 (Y axis = (*uaDf5:*WT day x -*uaDf5:*WT day 1)/(*uaDf5:*WT day 1)). For *glp-1(q231ts), fem-*

746 *3(q20ts),* and *glp-4(bn2ts),* 15°C is the permissive temperature (germline development occurs)

747 and 25°C is the restrictive temperature (female germline development is inhibited). Statistical

748 analysis was performed using one-way ANOVA with Tukey correction for multiple comparisons.

749 (*** $p < 0.001$, ** $p < 0.01$, * $p < 0.05$, . $p < 0.1$). Error bars represent SEM. **(C)** Analysis of the

750 molar ratio of mtDNA^{uaDf5} in aging adults (P0 adult) and their L1 progeny (F1 L1) in various nuclear

751 backgrounds shows that all strains decrease the *uaDf5* load during transmission from mother to

752   offspring, and that strains with significantly higher mtDNA^{uaDf5} levels (*atfs-1(et15), ced-*

753   *10(n1993)*, and *ced-13(sv32)*) have a more significant removal mechanism at day 4 of adulthood.

754   n=3 or more replicates of 200 worm populations were performed for each timepoint. Error bars

755   represent SEM. Grey dashed line indicates a hypothetical threshold at which high mtDNA^{uaDf5}

756   burden activates enhanced intergenerational purifying selection in older mothers. **(D)** Analysis

757   of the measured loss of mtDNA^{uaDf5} between mother and offspring at each day of adulthood

758   shows that mtDNA^{uaDf5} removal occurs. n=6 replicates of 200 worm populations for each

759   condition.

760
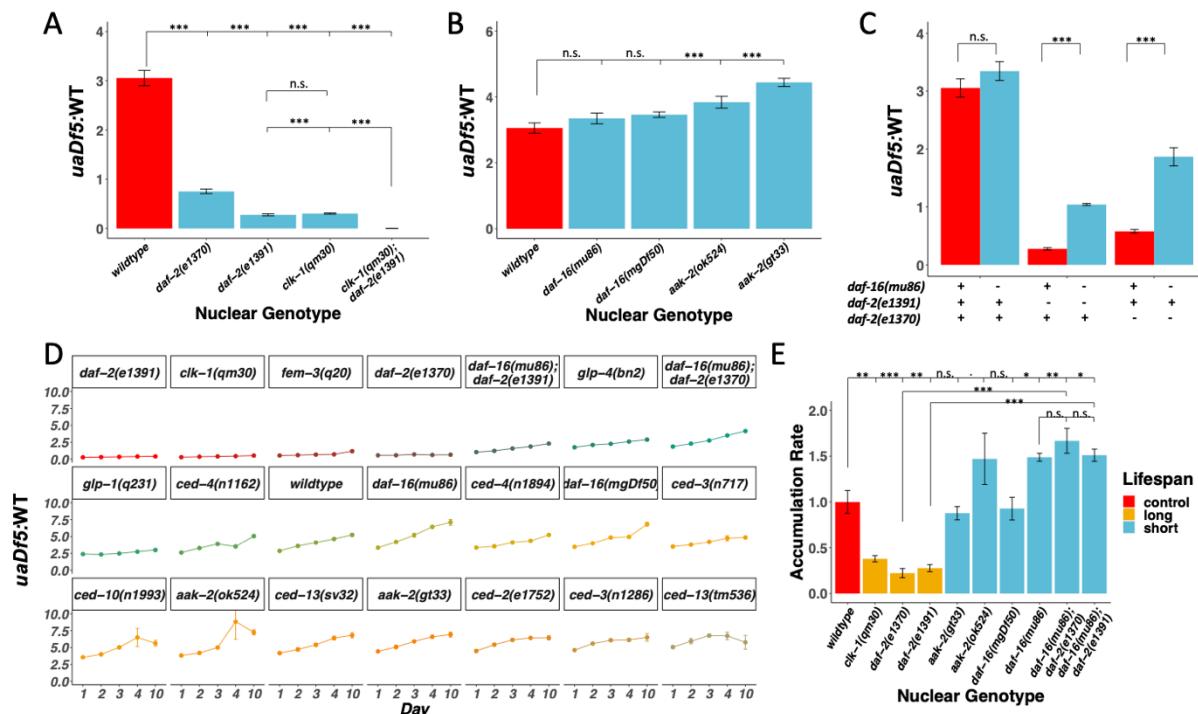
Figure 4

Figure 4: Lifespan mutants have both a lower steady-state level and accumulation rate of mtDNA^{uaDf5}. (A-C) Analysis of molar ratio of mtDNA^{uaDf5} in day 1 adults of various mutant backgrounds. **(A)** Analysis of steady-state mtDNA^{uaDf5} levels in long-lived mutants. **(B)** Analysis of steady-state mtDNA^{uaDf5} levels in short-lived mutants, showing synergistic activity on mtDNA^{uaDf5} removal capacity in the *daf-2(e1391) clk-1(qm30)* double mutant. **(C)** Analysis of steady-state mtDNA^{uaDf5} levels in *daf-2(-)* single and *daf-16(-); daf-2(-)* double mutants, showing a partial rescue of *daf-2(-)* phenotype by *daf-16(-)*. **(D)** Analysis of the molar ratio of mtDNA^{uaDf5} in aging adults in 21 different nuclear backgrounds shows a consistent accumulation trend. **(E)** Summary of the rate of increase for the lifespan regulation mutants, showing that *daf-16* rescues the *daf-2* accumulation rate phenotype. The normalized accumulation rate was calculated by fitting a regression line for each trial and then dividing the slope of the regression line by the slope of the averaged regression line found in a wildtype background. For **all**, n=3 or more replicates of 200

41

775   worm populations for each genotype and stage. For **A and E,** statistical analysis was performed

776   using one-way ANOVA with Tukey correction for multiple comparisons. For **C**, statistical analysis

777   was performed using one-way ANOVA. For **B**, statistical analysis was performed using one-way

778   ANOVA with Dunnett's correction for multiple comparisons. Error bars represent SEM. (*** $p <$

779   0.001, ** $p < 0.01$, * $p < 0.05$, . $p < 0.1$, n.s. not significant).

780

781   **Figure 5**
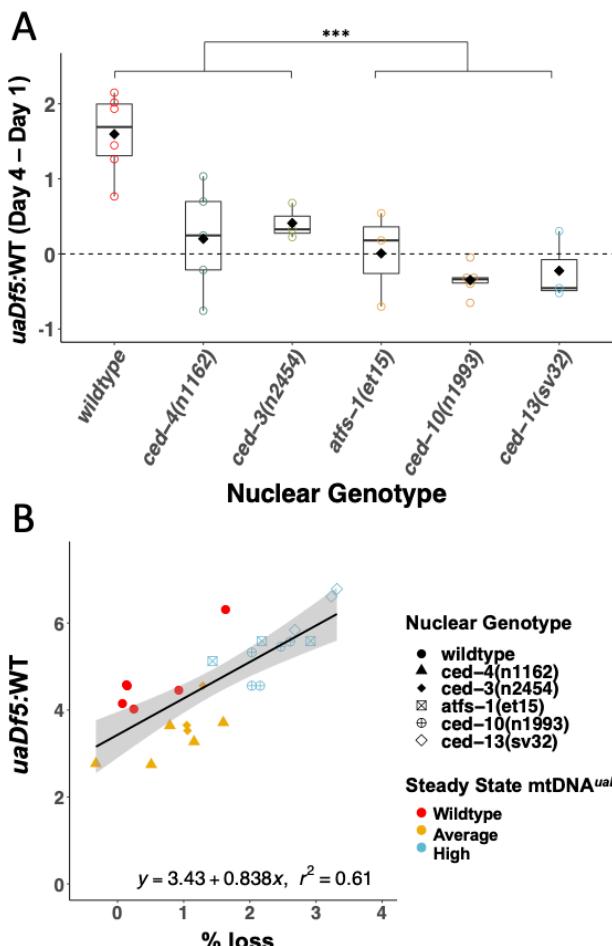
782
783   **Figure 5: Evidence for late adulthood-specific mechanisms for removal of mtDNA^{uaDf5}**

784   **(A)** Subtracting *uaDf5:*WT in progeny from day 1 adults from progeny of day 4 adults shows that

785   day 4 F1-L1s tend to have higher mtDNA^{uaDf5} burden than their day 1 siblings, but this is no longer

786   the case in nuclear backgrounds that result in a significantly higher steady-state levels of

787   mtDNA^{uaDf5} in the adult. n=3 or more replicates for each genotype and statistical analysis was

788   performed using the Mann-Whitney test. **(B)** Comparison of the molar ratio of mtDNA^{uaDf5} in day

789   4 adult mothers to the absolute % removal of mtDNA^{uaDf5} from mother to offspring shows a

790   positive correlation. (*** $p < 0.001$).

791
792

43

793   **Figure 6**
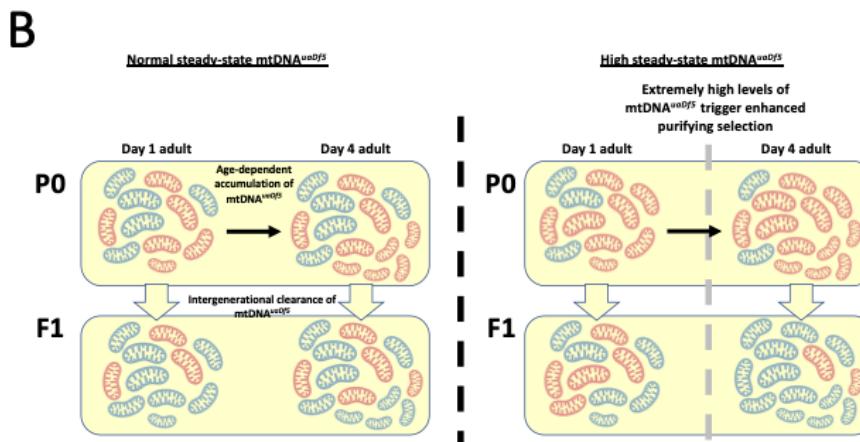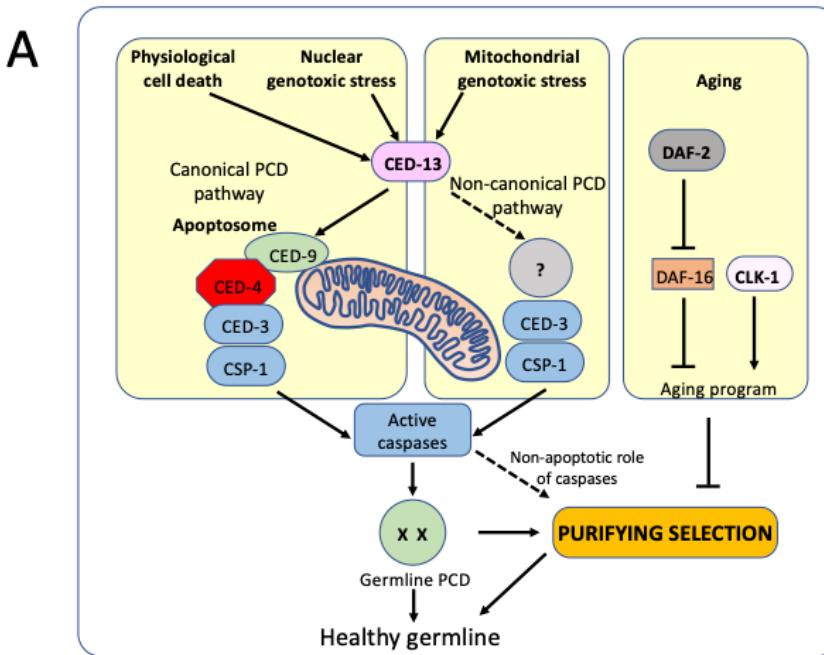
794
795   **Figure 6: Regulation of mtDNA^{uaDf5} accumulation and transmission by the PCD and aging**

796   **pathways**

797   **(A)** Our results suggest that CED-3 and CSP-1, which are activated by BH-3 only protein CED-13,

798   function cooperatively to promote mitochondrial purifying selection, independent of CED-9 and

799   the CED-4 apoptosome. The clearance of mtDNA^{uaDf5} may therefore involve induction of a non-

800   canonical germline PCD mechanism or non-apoptotic action of the CED-13/caspase axis.

801   Additionally, IIS and CLK-1 aging pathways act synergistically to regulate mitochondrial purifying

44

802   selection. **(B)** mtDNA^{uaDf5} (red) accumulates in the germline relative to mtDNA^{WT} (blue) as adults

803   age and the increased mtDNA^{uaDf5} levels are transmitted to the progeny, although the mtDNA^{uaDf5}

804   burden is consistently lower in progeny than mothers. This intergenerational purifying selection

805   is enhanced in the older mothers of mutants with high steady-state mtDNA^{uaDf5} (e.g., *ced-13*, *ced-*

806   *10,* and *atfs-1*), suggesting a threshold beyond which a germline PCD-independent mtDNA quality

807   control process may be initiated or enhanced in these older mothers.

808   **Supplemental Materials**

809   **Fig. 1 – figure supplement 1**

A

B

Sample	Allele	Total reads	Variant reads	% variant
A	*uaDf5*	858.40*	658.48*	76.71
	w47	631	472	72.62
B	*uaDf5*	451.54*	347.51*	76.96
	w47	339	248	71.06

C

Complex:	I	II	III	IV	V
nDNA-encoded	~30	~8	4	~6	~13
mtDNA-encoded	7	1	0	3	1

D

E

810

46
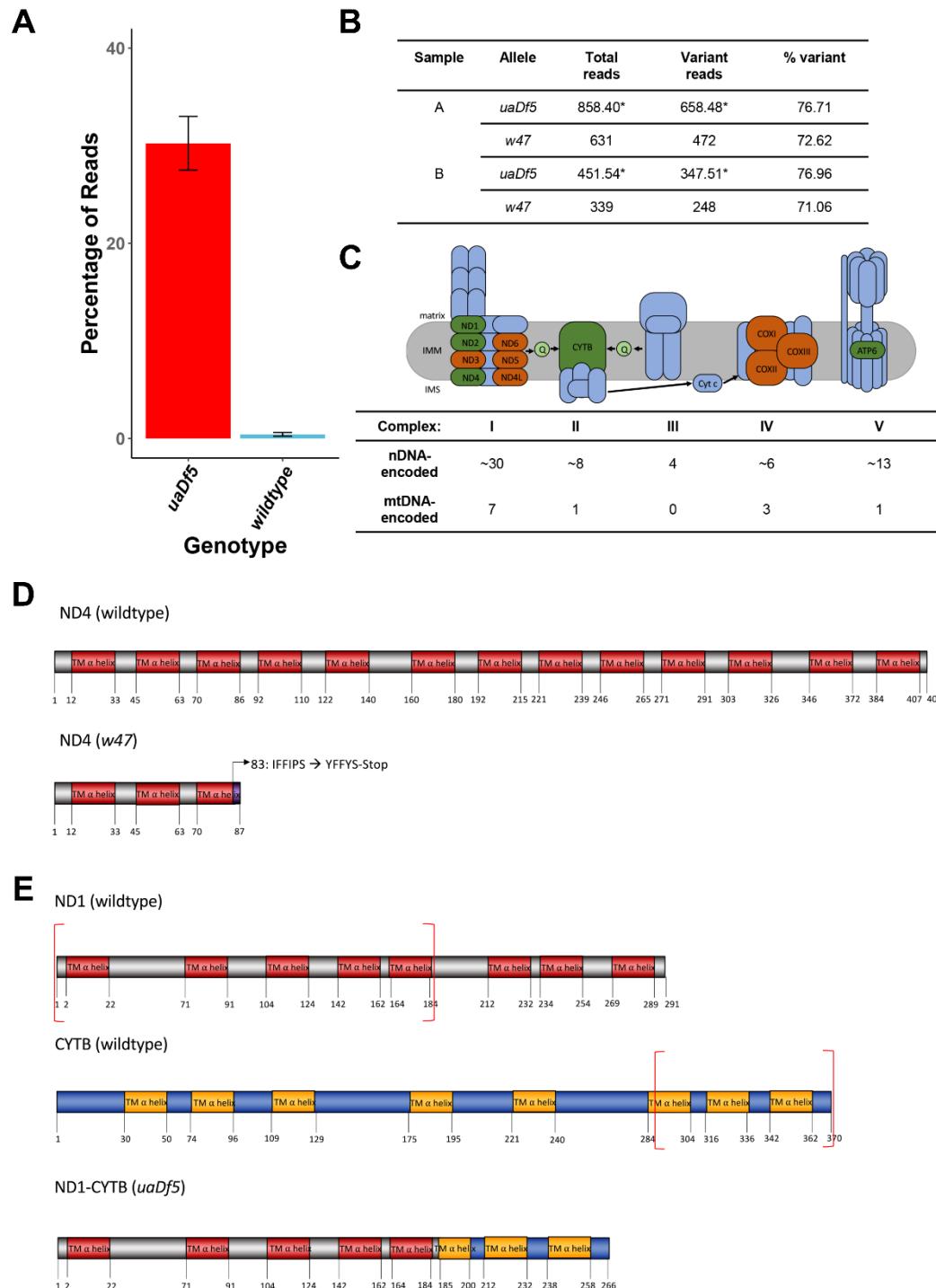
811   **Fig. 1 – figure supplement 1: Characterization of the *uaDf5* allele. (A)** The percentage of reads

812   that mapped to the *w47* insertion in *uaDf5* samples (red) and wildtype samples (blue). Error bars

813   represent SEM. **(B)** Table outlining the percentage of reads that mapped to the *w47* and *uaDf5*

814   mutations in *uaDf5* samples. The number of variant reads was determined by averaging the

815   mapped reads across the deleted region and subtracting that from the average number of reads

816   mapped to the rest of the mtDNA genome (total reads). **(C)** Diagram showing the mitochondrial

817   respiratory chain (MRC) machinery subunits. Blue indicates nDNA-encoded subunits, orange and

818   green indicate mtDNA-encoded subunits. Green indicates those subunits that are knocked out in

819   the *uaDf5* allele (including ND4 which is knocked out by the linked *w47* mutation). **(D)** Diagram

820   showing the likely effect of the *w47* mutation on ND4 protein translation. ND4 is a 409-aa long

821   transmembrane subunit that spans the inner mitochondrial membrane 13 times. The *w47*

822   mutation results in a premature stop codon at position 89, eliminating 10 of the 13 alpha-helix

823   membrane domains. **(E)** Diagram showing the likely effect of the *uaDf5* mutation on ND1 protein

824   translation. ND1 is a 291-aa long transmembrane subunit that spans the inner mitochondrial

825   membrane 8 times and CYTB is a 370-aa long transmembrane subunit that spans the inner

826   mitochondrial membrane 8 times. The *uaDf5* mutation results in a 266 amino acid long fusion

827   protein that connects the first 185 amino acids (and 5 subunits) of ND1 with the last 81 amino

828   acids (and 3 subunits) of CYTB.

829

830 **Fig. 1 – figure supplement 2**
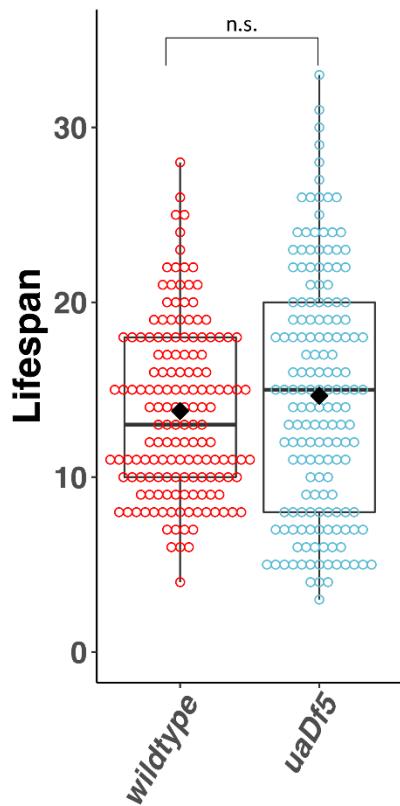
831

832 **Fig. 1 – figure supplement 2: Lifespan analysis of the impact of *uaDf5*.** Lifespan analysis of N2

833 bearing *uaDf5* compared to wildtype N2. Day 1 is defined as the day starved L1s are plated on

834 food. Box plots show median and IQR, and the diamond indicates the mean. Statistical analysis

835 was performed using the Mann-Whitney test. (n.s. not significant).

836

48

837 **Fig. 2 – figure supplement 1**
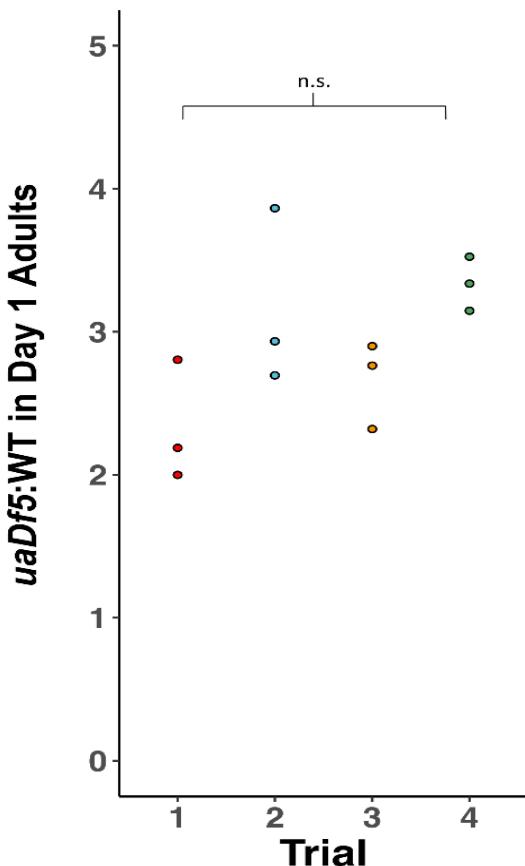
838

839 **Fig. 2 – figure supplement 1: Reproducibility of ddPCR measurement of *uaDf5*.** Analysis of the

840 steady-state of *uaDf5* in a wildtype nuclear background shows highly stable steady-state levels.

841 Trials were done months apart on different thaws. Dots represent biological replicates. Statistical

842 analysis was performed using one-way ANOVA with Tukey correction for multiple comparisons.

843 (n.s. not significant).

844

845 **Fig. 2 – figure supplement 2**
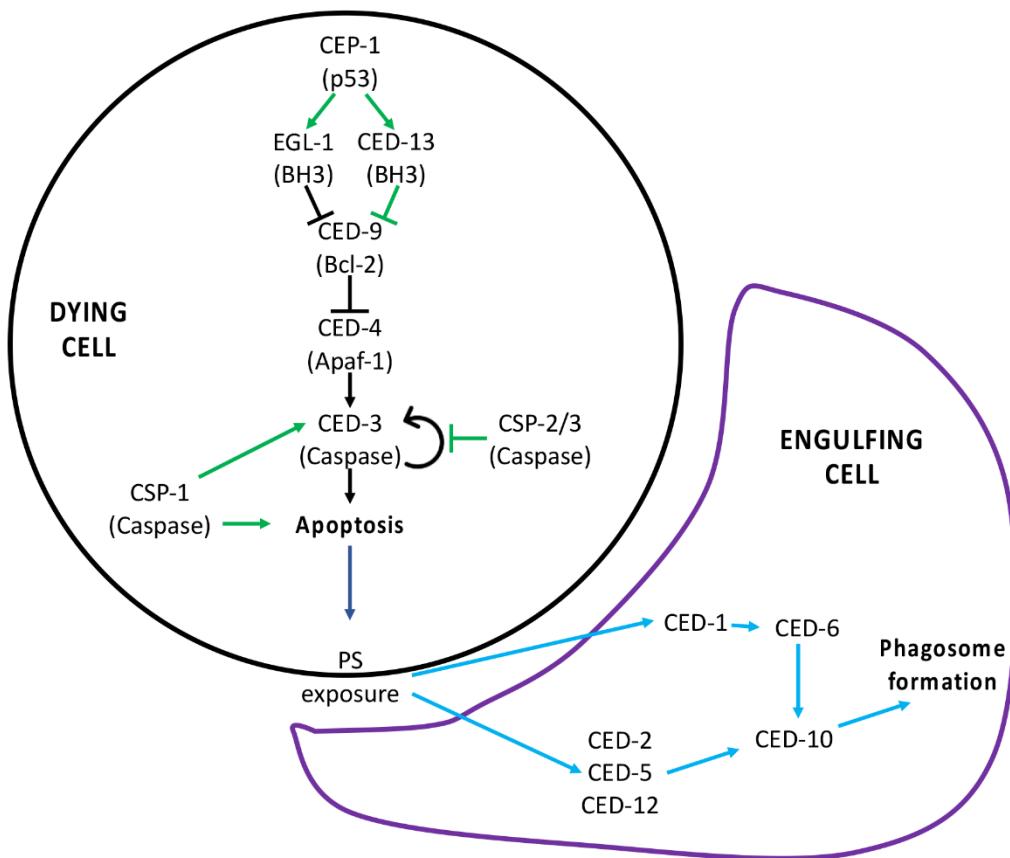
846

847

848 **Fig. 2 – figure supplement 2: PCD Signaling pathway. (A)** Signaling pathway for programmed cell

849 death. The canonical pathway is shown with black arrows, the noncanonical pathway is shown

850 with green arrows, and the downstream engulfment pathway is shown with blue arrows.

851 Adapted from [38].

852

853   **Fig. 2 – figure supplement 3**

A

Allele	Location	Domain	Level of *uaDf5*
n1286	W428opal	p15	highest
n717	Position 403 - Exon 7 acceptor	p15	high
n2454	A466T	p15	unchanged
n718	G65R	Prodomain	low

B
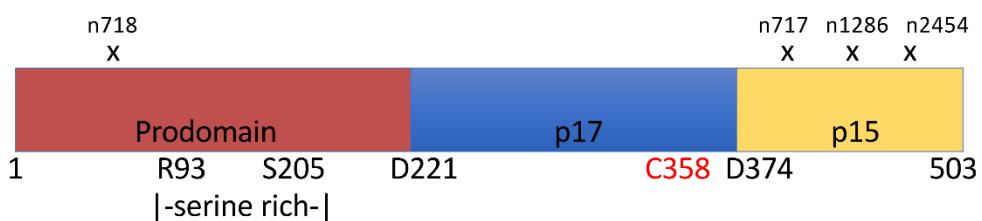
854

855   **Fig. 2 – figure supplement 3: Analysis of the *ced-3* alleles. (A)** Locations and consequences of

856   the four tested *ced-3* alleles, as well as the measured fractional abundance of *uaDf5*. **(B)** Diagram

857   showing the locations of the mutations for each allele.

858

859   **Fig. 2 – figure supplement 4**
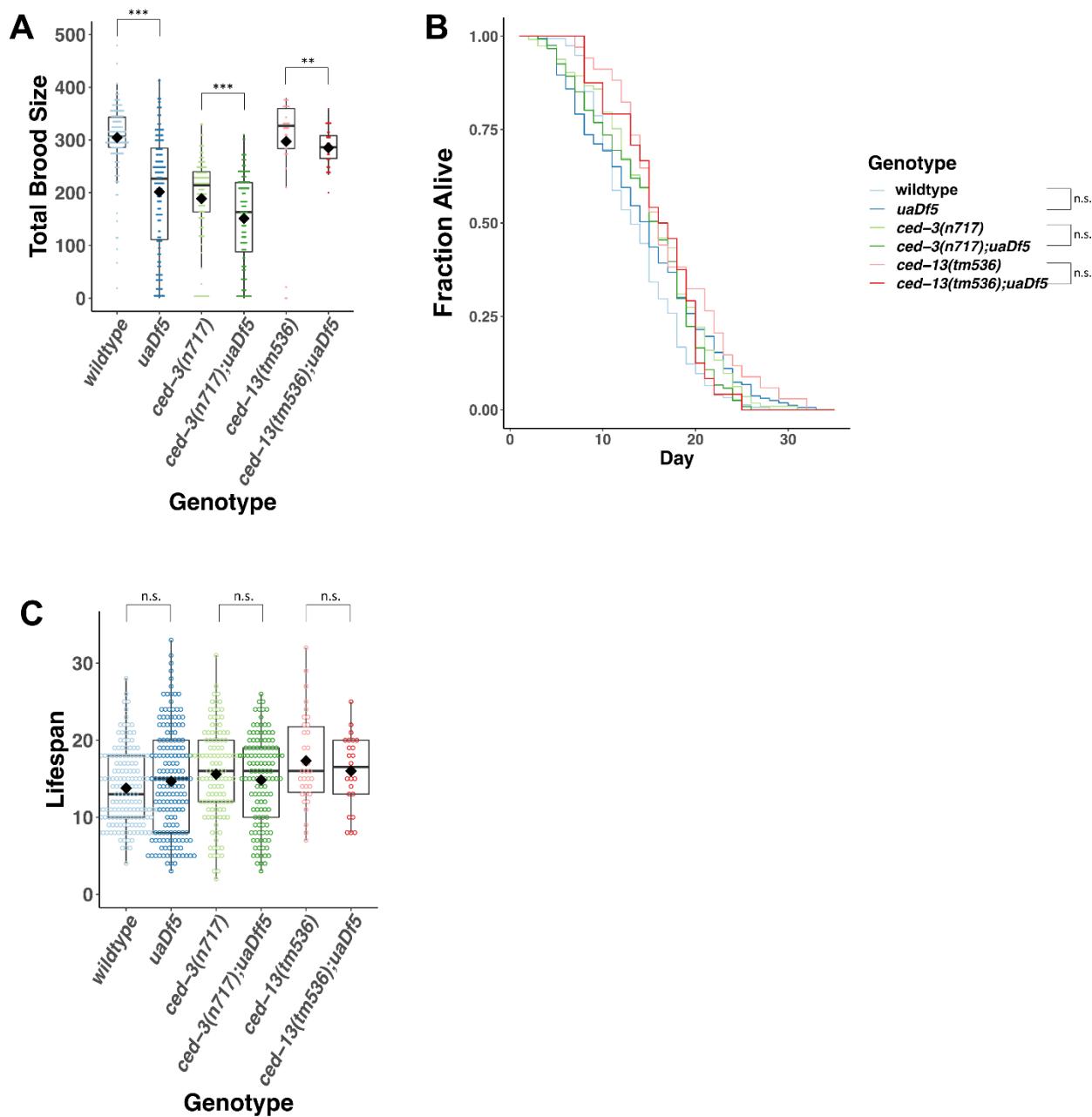
860

861   **Fig. 2 – figure supplement 4: Analysis of the impact of *uaDf5* on fitness parameters in PCD**

862   **mutants. (A)** Brood size analysis of PCD mutants. **(B)** Lifespan analysis shows that *uaDf5* does not

863   affect lifespan in both wildtype background and in PCD mutant backgrounds. **(C)** Lifespan analysis

864   shows that *uaDf5* does not affect lifespan in a wildtype nuclear background nor in PCD mutant

52

865   backgrounds. For **B and C,** day 1 is defined as the day starved L1s are plated on food. For **A and**

866   **C**, box plots show median and IQR, and the diamond indicates the mean. Statistical analysis was

867   performed using the Mann-Whitney Wilcoxon test. (*** $p < 0.001$, ** $p < 0.01$, * $p < 0.05$, . $p <$

868   0.1, n.s. not significant).

869

870

871   **Fig. 3 – figure supplement 1**
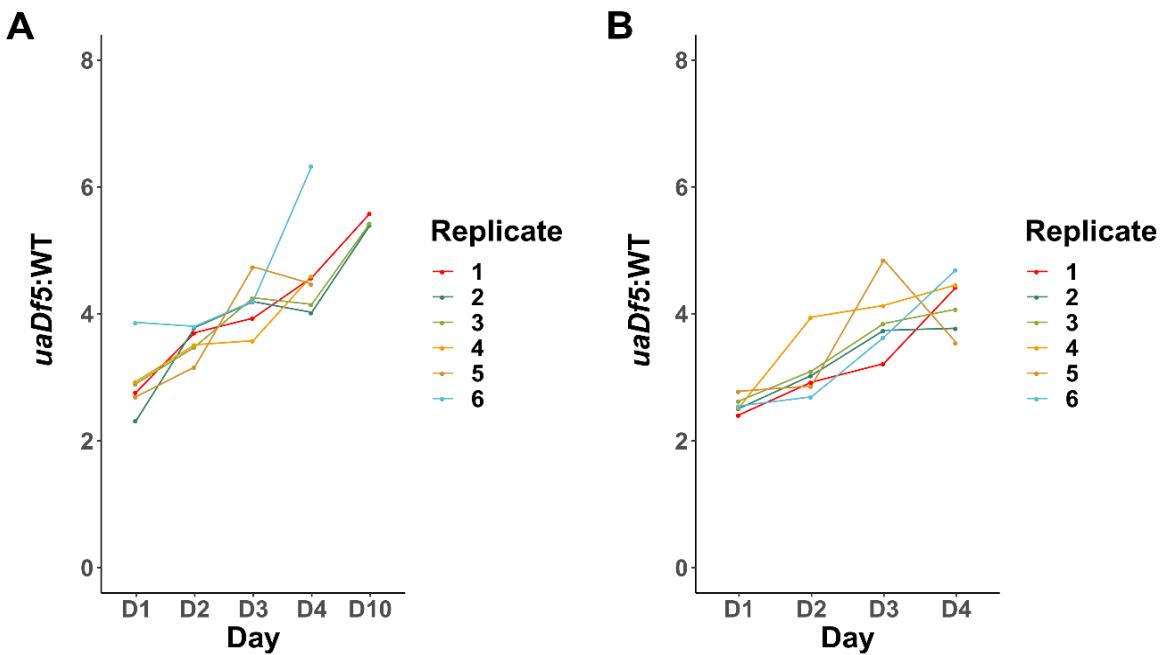
872

873   **Fig. 3 – figure supplement 1: *uaDf5* accumulation in individual lines of adults and progeny. (A)**

874   Analysis of *uaDf5* accumulation in individual lines of aging P0 adults shows a consistent

875   accumulation trend as adults age. **(B)** Analysis of *uaDf5* accumulation in individual lines of F1-L1

876   progeny that were born from those mothers shown in panel A show a consistent trend of progeny

877   born from older mothers inheriting a larger *uaDf5* load than their siblings born from younger

878   mothers.

879

880 **Fig. 4 – figure supplement 1**
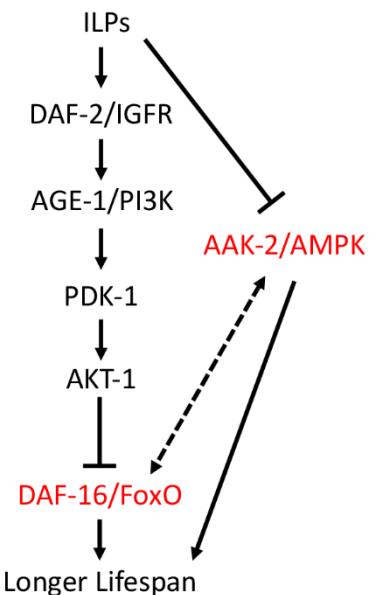
881

882 **Fig. 4 – figure supplement 1: IIS Signaling pathway.** Insulin-like peptides (ILPs) bind to DAF-2 and

883 activate the PI3P pathway which prevents nuclear translocation of DAF-16. AAK-2 may

884 phosphorylate and activate DAF-16 transcriptional activity. Loss of *aak-2* or *daf-2* (highlighted in

885 red) reduces lifespan

886

887   **Fig. 4 – figure supplement 2**
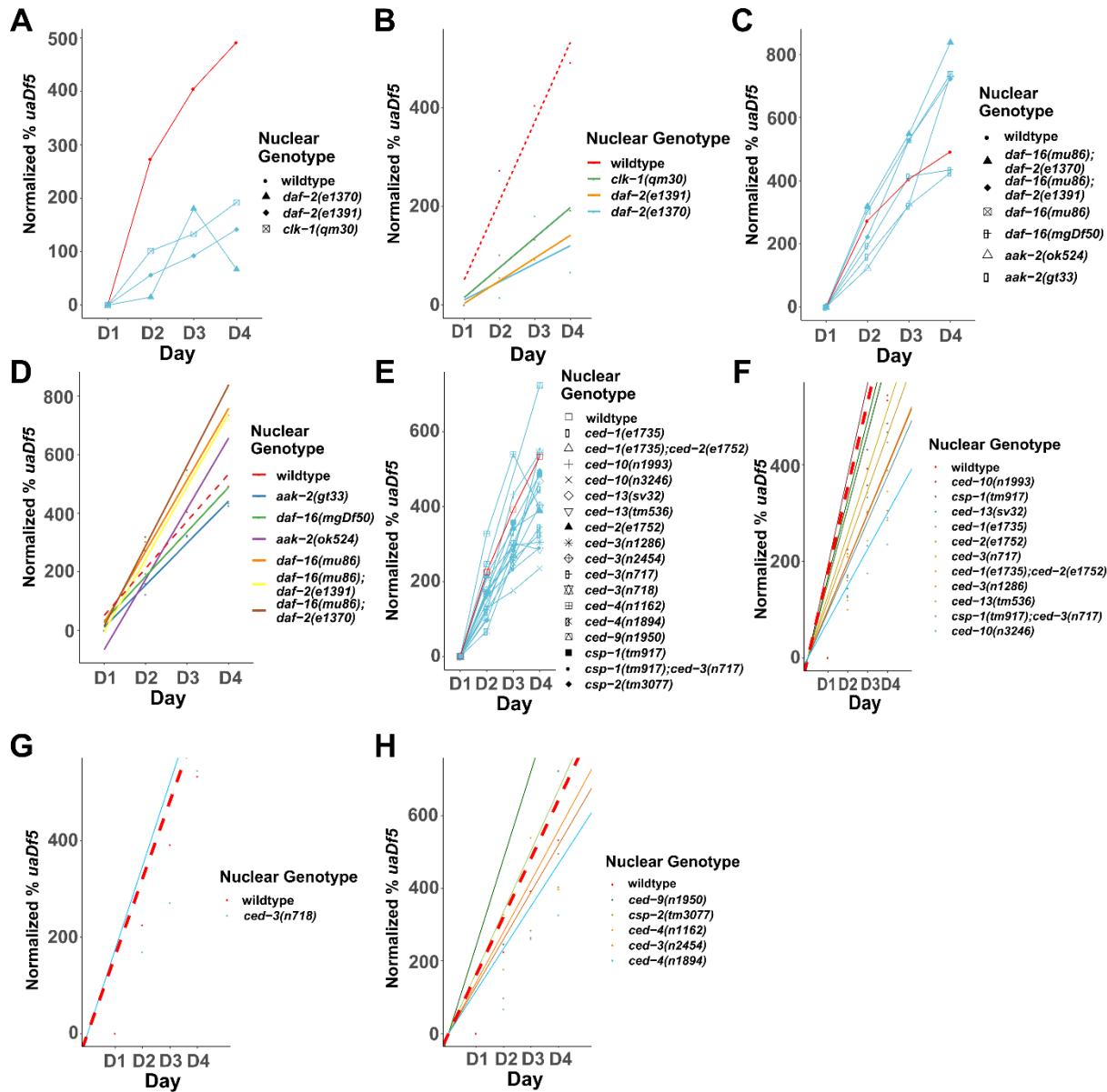
888

889   **Fig. 4 – figure supplement 2: Analysis of the accumulation of mtDNA^{uaDf5} in PCD and lifespan**

890   **mutants.** Analysis of the normalized fractional abundance *uaDf5* [(% *uaDf5* day x- % *uaDf5* day

891   1)* % *uaDf5* day 1] in steady-state populations, showing the accumulation rate of mtDNA^{uaDf5} as

892   worms age from day 1 to day 4 of adulthood. **(A)** Analysis of the accumulation of *uaDf5* in long-

893   lived mutants. **(B)** Analysis of the accumulation of mtDNA^{uaDf5} in short-lived mutants. **(C-D)**

894   Linear regression analysis of the normalized fractional abundance *uaDf5* [(% *uaDf5* day x- %

895   *uaDf5* day 1)* % *uaDf5* day 1] in steady-state populations, showing the accumulation rate of

896   mtDNA^{uaDf5} as worms age from day 1 to day 4 of adulthood. **(C)** Analysis of long-lived mutants.

897   **(D)** Analysis of short-lived mutants. **(E)** Analysis of the accumulation of mtDNA^{uaDf5} in PCD

898   mutants. **(F-H)** Linear regression analysis of the normalized fractional abundance mtDNA^{uaDf5}

899   [(% *uaDf5* day x- % *uaDf5* day 1)* % *uaDf5* day 1] in steady-state populations, showing the

900   accumulation rate of mtDNA^{uaDf5} as worms age from day 1 to day 4 of adulthood. **(F)** Analysis of

901   PCD mutants with significantly high steady-state level of mtDNA^{uaDf5}. **(G)** Analysis of PCD

902   mutants with significantly low steady-state level of mtDNA^{uaDf5}. **(H)** Analysis of PCD mutants

903   with no significant change in the steady-state level of mtDNA$^{uaDf5.}$ For **C, D, F, G, and H** dots

904   represent actual datapoints, lines are fitted regression models of the data. For all, n=3

905   replicates or more of 200 worm populations for each datapoint.

906

907

908   **Fig. 4 – figure supplement 3**
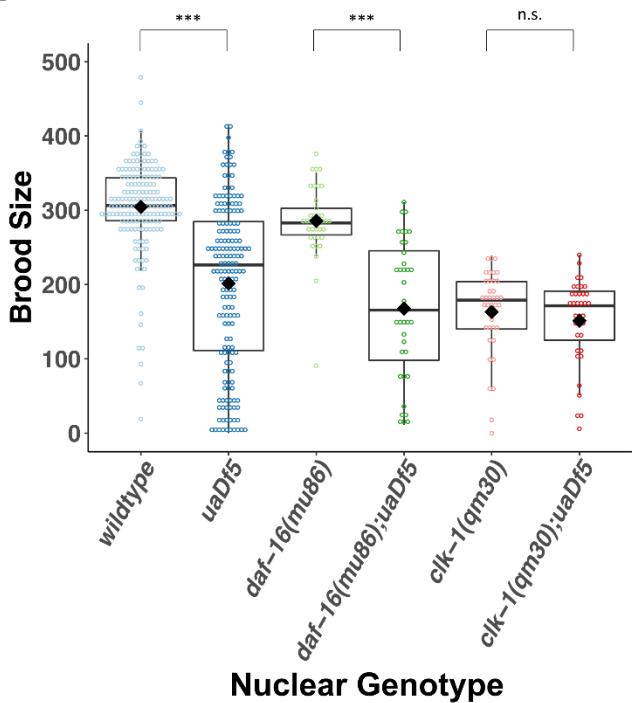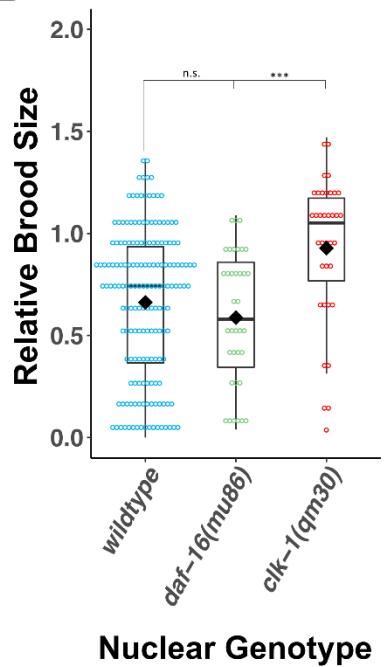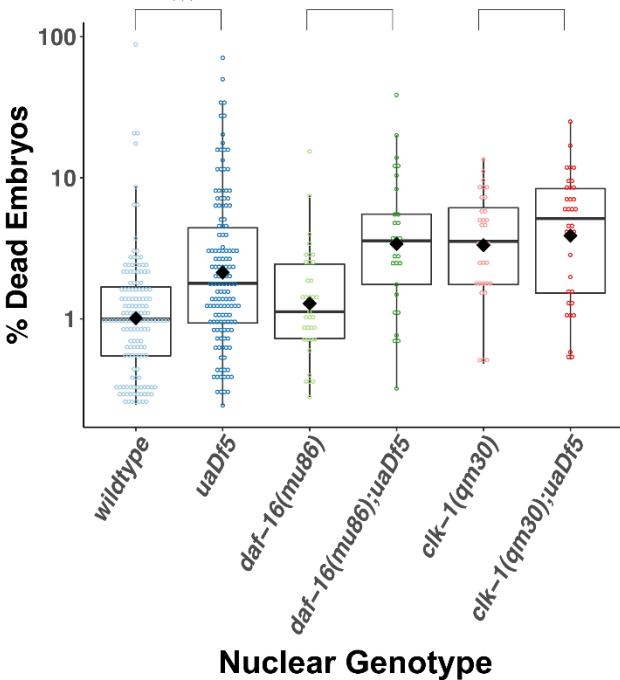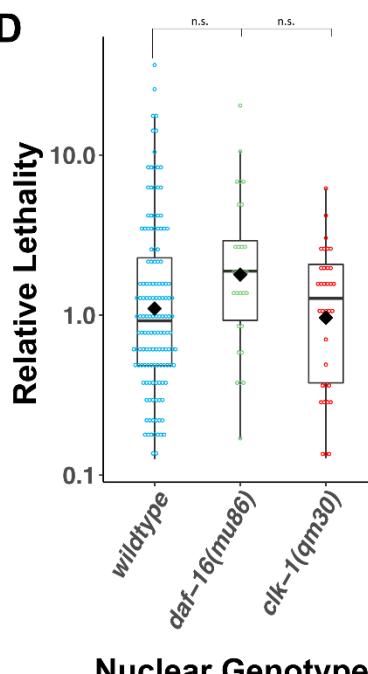
909

910   **Fig. 4 – figure supplement 3:** *uaDf5* **differentially impacts fitness parameters in lifespan-**

911   **affecting mutants. (A-B)** Brood size analysis showing how *uaDf5* differentially impacts brood size

58

912   in lifespan mutant backgrounds. *uaDf5* has no negative impact on the long-lived mutant *clk-1* but

913   has a modestly larger negative impact on the short-lived mutant *daf-16* than it does in the

914   wildtype background. **(B)** Relative brood size of the animals with and without *uaDf5* in the

915   indicated mutant backgrounds. **(C-D)** Embryonic lethality analysis showing how *uaDf5*

916   differentially impacts embryonic lethality in lifespan mutant backgrounds. *uaDf5* has no negative

917   impact on the long-lived mutant *clk-1* but has a modestly larger negative impact on the short-

918   lived mutant *daf-16* than it does in a wildtype background. **(D)** Relative lethality of the animals

919   with and without *uaDf5* in the indicated mutant backgrounds. Box plots show median and IQR,

920   and the diamond indicates the mean. For **A and C**, statistical analysis was performed using the

921   Mann-Whitney test. For **B and D**, statistical analysis was performed using the Kruskal-Wallis test.

922   (*** $p < 0.001$, ** $p < 0.01$, * $p < 0.05$, . $p < 0.1$, n.s. not significant).

923

924 **Supplementary Table 1:** A summary of all mutants analyzed in the PCD pathway, including their

925 known homologs, whether they are part of the core PCD machinery, if they are pro-apoptotic or

926 anti-apoptotic, whether they are mitochondrial proteins, and molecular details of the alleles

927 analyzed.

Gene	Homolog	Core Machinery	Role in Apoptosis	Mitochondrial?	Allele	Parental Strain	Molecular Nature of the Allele	Protein Change
ced-1	SCARF2	N	Pro(engulfment)	N	e1735	CB3203	Substitution	Nonsense Q→Ochre
ced-2	CRK	N	Pro(engulfment)	N	e1752	CB3257	Substitution	Nonsense W→Opal
ced-3	CASPASE	Y	Pro(executor caspase)	N	n717	MT1522	Substitution	Splice site C→T
					n1286	MT3002	Substitution	Nonsense W→Opal
					n718	MT1743	Substitution	Missense G→R
					n2454	MT8354	Substitution	Missense A→T
ced-4	APAF1	Y	Pro(apoptosome)	Y/N (primarily nuclear membrane)	n1162	MT2547	Substitution	Nonsense Q→Ochre
					n1894	MT5287	Not curated	Unknown
ced-9	BCL2	Y	Anti	Y	n1950	MT4770	Substitution	Missense G→E
ced-10	RAC	N	Pro(engulfment)	N	n1993	MT5013	Substitution	Missense V→G
					n3246	MT9958	Substitution	Missense G→R
ced-13	BH3	N	Pro	N	tm536	FX536	523bp deletion	Only first 17bp remain
					sv32	MD792	1304bp deletion	Complete knockout, also inx-5
csp-1	CASPASE	N	Pro(caspase)	N	tm917	JR3196	751bp deletion	Only first 59bp remain
csp-2	CASPASE	N	Anti	N	tm3077	JR3397	319bp deletion	Start at position 7317, deletes parts of exon 13

60

								and all of 14

928

929

930 **Supplementary Table 2:** A summary of all lifespan mutants analyzed, including their known

931 homologs, cellular pathways they are known to act in, whether the mutant extends or reduces

932 lifespan, and molecular details of the alleles analyzed.

Gene	Homologs	Pathway	Allele	Parental Strain	Molecular Nature of the Allele	Protein Change	Mutant lifespan	Note
aak-2	AMPK	IIS pathway, adult lifespan, peptidyl-serine phosphorylation, regulation of protein localization	gt33	TG38	606bp deletion	Starts at position 3979, deletes exon 3	Decrease	-
			ok524	RB754	408bp deletion	Starts at position 4136, deletes part of exon 3	Decrease	-
clk-1	COQ7	Adult behavior, regulation of cellular metabolism	qm30	MQ130	590bp deletion	Starts at position 1044, deletes part of exon 4 and 5	Increase	-
daf-2	IGFR	IIS pathway, cellular response to salt, negative regulator of macromolecule metabolic processes, positive regulation of developmental growth	e1391	DR1574	Substitution	Missense P→L	Increase	ts
			e1370	CB1370	Substitution	Missense P→S	Increase	ts
			m41	DR1564	Substitution	Missense G→E	Increase	ts
daf-16	FOXO	IIS pathway, defense response to bacterium, regulation of cellular biosynthetic process, regulation of post-	mu86	CF1038	1098bp deletion	Deletes 5 exons	Decrease	-
			mgDf50	GR1307	20193bp deletion with TCTTCATTTTCAG insertion	Deletes 7 exons	Decrease	-

62

		embryonic development						
fem-3	novel	Male somatic sex determination, masculinization of hermaphrodite germline, positive regulation of macromolecule metabolic process	*q20*	JK816	Not curated	Unknown	Increase	Gof and ts; female germline development inhibited
glp-4	VARS	Cell fate specification, embryonic pattern specification, positive regulation of cell proliferation	*bn2*	SS104	Substitution	Missense G→D	Increase	ts; germline development inhibited

933

934

935   **Supplementary Table 3:** *C. elegans* strains used in this study.

Strain	Genotype	Source
N2	wildtype	CGC
LB138	*him-8(e1489) IV; uaDf5/+*	CGC
JR3630	*N2; uaDf5/+ (8x backcross version of LB138, him(e1489) was outcrossed)*	This study
JR3688	*pink-1(tm1779); uaDf5/+*	This study
JR3880	*ced-3(n717) IV; uaDf5/+*	This study
JR4330	*csp-1(tm917) II; uaDf5/+*	This study
JR3977	*ced-3(n1286) IV; uaDf5/+*	This study
JR3955	*ced-13(sv32) X; uaDf5/+*	This study
JR3976	*ced-13(tm536) X; uaDf5/+*	This study
JR3926	*ced-10(n1993) IV; uaDf5/+*	This study
JR4001	*ced-10(n3246) IV; uaDf5/+*	This study
JR3972	*ced-1(e1735) I; uaDf5/+*	This study
JR3978	*ced-2(e1752) IV; uaDf5/+*	This study
JR4010	*ced-1(e1735)I; ced-2(e1752)IV; uaDf5/+*	This study
JR3938	*ced-3(n2454) IV; uaDf5/+*	This study
JR3925	*ced-4(n1162) III; uaDf5/+*	This study
JR4017	*ced-4(n1894) III; uaDf5/+*	This study
JR3986	*csp-2(tm3077) IV; uaDf5/+*	This study
JR4027	*ced-9(n1950) III; uaDf5/+*	This study
JR3983	*ced-3(n718) IV; uaDf5/+*	This study
MT1522	*ced-3(n717) IV*	CGC
FX536	*ced-13(tm536) X*	CGC
JR3966	*glp-4(bn2) I; uaDf5/+*	This study
JR3949	*fem-3(q20) IV; uaDf5/+*	This study
JR3937	*atfs-1(et15) V; uaDf5/+*	This study
JR3960	*daf-2(e1370) III; uaDf5/+*	This study
JR3963	*daf-2(e1391) III; uaDf5/+*	This study
JR3993	*clk-1(qm30) III; uaDf5/+*	This study
JR4060	*daf-2(e1391) clk-1(qm30) III; uaDf5/+*	This study
JR3995	*daf-16(mu86) I; uaDf5/+*	This study
JR3997	*daf-16(mgDf50) I; uaDf5/+*	This study
JR4011	*aak-2(ok524) X; uaDf5/+*	This study
JR4012	*aak-2(gt33) X; uaDf5/+*	This study
JR4008	*daf-16(mu86) I; daf-2(e1391) III; uaDf5/+*	This study
JR4005	*daf-16(mu86) I; daf-2(e1370) III; uaDf5/+*	This study
JR3941	*glp-1(q231) III; uaDf5/+*	This study
CF1038	*daf-16(mu86) I*	CGC
MQ130	*clk-1(qm30) III*	CGC

| JR3981 | *csp-1(tm917) II; ced-3(n717) IV; uaDf5/+* | This study |

936

937

Acknowledgments

Competing Interests

944   The authors declare no competing or financial interests.

Author contributions

947   Sagen E. Flowers - conceptualization, investigation, funding acquisition, writing – original draft

948   preparation, writing – review and editing

949   Rushali Kothari – investigation, writing – review and editing

950   Yamila N. Torres Cleuren - investigation, writing – review and editing

951   Melissa R. Alcorn – statistics, writing – review and editing

952   Chee Kiang Ewe - writing – review and editing

953   Geneva Alok - writing – review and editing

954   Pradeep M. Joshi – conceptualization, investigation, writing – review and editing

955   Joel H. Rothman - conceptualization, supervision, funding acquisition, writing – review and

956   editing

Funding

960 **Data Availability**

961 All data generated or analyzed during this study are included in this article and accompanied

962 supplementary materials. The raw reads of the sequenced N2, LB138, and JR3688 genomes

963 have been deposited at the NCBI SRA under the study accession number PRJNA836592.

964 **References**

965 1. YS N, DM T. Mitochondrial disease: genetics and management. J Neurol. J Neurol;

966   2016;263: 179–191. doi:10.1007/S00415-015-7884-3

967 2. PF C. Mitochondrial disease in adults: what's old and what's new? EMBO Mol Med.

968   EMBO Mol Med; 2015;7: 1503–1512. doi:10.15252/EMMM.201505079

969 3. Gorman GS, Schaefer AM, Ng Y, Gomez N, Blakely EL, Alston CL, et al. Prevalence of

970   nuclear and mitochondrial DNA mutations related to adult mitochondrial disease. Ann

971   Neurol. John Wiley & Sons, Ltd; 2015;77: 753–759. doi:10.1002/ANA.24362

972 4. Ghaoui R, Sue CM. Movement disorders in mitochondrial disease. J Neurol. Dr. Dietrich

973   Steinkopff Verlag GmbH and Co. KG; 2018;265: 1230–1240. doi:10.1007/s00415-017-

974   8722-6

975 5. Area-Gomez E, Schon EA. Mitochondrial genetics and disease. Journal of Child Neurology.

976   SAGE Publications Inc.; 2014. pp. 1208–1215. doi:10.1177/0883073814539561

977 6. Dhillon VS, Fenech M. Mutations that affect mitochondrial functions and their

978   association with neurodegenerative diseases. Mutation Research - Reviews in Mutation

979   Research. 2014. pp. 1–13. doi:10.1016/j.mrrev.2013.09.001

980 7. Park CB, Larsson NG. Mitochondrial DNA mutations in disease and aging. Journal of Cell

981   Biology. 2011. pp. 809–818. doi:10.1083/jcb.201010024

67

982   8.   Burté F, Carelli V, Chinnery PF, Yu-Wai-Man P. Disturbed mitochondrial dynamics and

983   neurodegenerative disorders. Nature Reviews Neurology. Nature Publishing Group;

984   2015. pp. 11–24. doi:10.1038/nrneurol.2014.228

985   9.   Schon EA, Dimauro S, Hirano M. Human mitochondrial DNA: Roles of inherited and

986   somatic mutations. Nature Reviews Genetics. 2012. pp. 878–890. doi:10.1038/nrg3275

987   10.   Brown WM, George M, Wilson AC. Rapid evolution of animal mitochondrial DNA. Proc

988   Natl Acad Sci U S A. 1979;76: 1967–1971. doi:10.1073/pnas.76.4.1967

989   11.   Konrad A, Thompson O, Waterston RH, Moerman DG, Keightley PD, Bergthorsson U, et

990   al. Mitochondrial mutation rate, spectrum and heteroplasmy in Caenorhabditis elegans

991   spontaneous mutation accumulation lines of differing population size. Mol Biol Evol.

992   Oxford University Press; 2017;34: 1319–1334. doi:10.1093/molbev/msx051

993   12.   Denver DR, Morris K, Lynch M, Vassilieva LL, Thomas WK. High direct estimate of the

994   mutation rate in the mitochondrial genome of Caenorhabditis elegans. Science (80-).

995   2000;289: 2342–2344. doi:10.1126/science.289.5488.2342

996   13.   Palozzi JM, Jeedigunta SP, Hurd TR. Mitochondrial DNA Purifying Selection in Mammals

997   and Invertebrates. Journal of Molecular Biology. Academic Press; 2018. pp. 4834–4848.

998   doi:10.1016/j.jmb.2018.10.019

999   14.   Stewart JB, Freyer C, Elson JL, Larsson NG. Purifying selection of mtDNA and its

1000   implications for understanding evolution and mitochondrial disease. Nature Reviews

1001   Genetics. 2008. pp. 657–662. doi:10.1038/nrg2396

1002   15.   Twig G, Shirihai OS. The interplay between mitochondrial dynamics and mitophagy.

1003   Antioxidants and Redox Signaling. 2011. pp. 1939–1951. doi:10.1089/ars.2010.3779

68

1004   16.   Busch KB, Kowald A, Spelbrink JN. Quality matters: How does mitochondrial network

1005   dynamics and quality control impact on mtDNA integrity? Philosophical Transactions of

1006   the Royal Society B: Biological Sciences. Royal Society of London; 2014.

1007   doi:10.1098/rstb.2013.0442

1008   17.   Ni HM, Williams JA, Ding WX. Mitochondrial dynamics and mitochondrial quality control.

1009   Redox Biology. Elsevier B.V.; 2015. pp. 6–13. doi:10.1016/j.redox.2014.11.006

1010   18.   Ashrafi G, Schwarz TL. The pathways of mitophagy for quality control and clearance of

1011   mitochondria. Cell Death and Differentiation. 2013. pp. 31–42. doi:10.1038/cdd.2012.81

1012   19.   Youle RJ, Narendra DP. Mechanisms of mitophagy. Nat Rev Mol Cell Biol. 2011;12: 9–14.

1013   doi:10.1038/nrm3028

1014   20.   Tilokani L, Nagashima S, Paupe V, Prudent J. Mitochondrial dynamics: Overview of

1015   molecular mechanisms. Essays in Biochemistry. Portland Press Ltd; 2018. pp. 341–360.

1016   doi:10.1042/EBC20170104

1017   21.   Hernando-Rodríguez B, Artal-Sanz M. Mitochondrial Quality Control Mechanisms and the

1018   PHB (Prohibitin) Complex. Cells. MDPI AG; 2018;7: 238. doi:10.3390/cells7120238

1019   22.   Sté phane Rolland AG, Schneid S, Schwarz M, Mokranjac D, Lambie E, Conradt B.

1020   Compromised Mitochondrial Protein Import Acts as a Signal for UPR mt. Cell Rep.

1021   2019;28: 1659–1669. doi:10.1016/j.celrep.2019.07.049

1022   23.   Münch C. The different axes of the mammalian mitochondrial unfolded protein response.

1023   BMC Biology. BioMed Central Ltd.; 2018. doi:10.1186/s12915-018-0548-x

1024   24.   Callegari S, Dennerlein S. Sensing the stress: A role for the UPR mt and UPR am in the

1025   quality control of mitochondria. Frontiers in Cell and Developmental Biology. Frontiers

69

1026   Media S.A.; 2018. doi:10.3389/fcell.2018.00031

1027   25.   Gitschlag BL, Kirby CS, Samuels DC, Gangula RD, Mallal SA, Patel MR. Homeostatic

1028   Responses Regulate Selfish Mitochondrial Genome Dynamics in C. elegans. Cell Metab.

1029   Cell Press; 2016;24: 91–103. doi:10.1016/j.cmet.2016.06.008

1030   26.   Nargund AM, Pellegrino MW, Fiorese CJ, Baker BM, Haynes CM. Mitochondrial import

1031   efficiency of ATFS-1 regulates mitochondrial UPR activation. Science (80-). American

1032   Association for the Advancement of Science; 2012;337: 587–590.

1033   doi:10.1126/science.1223560

1034   27.   Lin YF, Schulz AM, Pellegrino MW, Lu Y, Shaham S, Haynes CM. Maintenance and

1035   propagation of a deleterious mitochondrial genome by the mitochondrial unfolded

1036   protein response. Nature. Nature Publishing Group; 2016;533: 416–419.

1037   doi:10.1038/nature17989

1038   28.   Murphy CT, Hu PJ. Insulin/insulin-like growth factor signaling in C. elegans [Internet].

1039   WormBook : the online review of C. elegans biology. 2013. pp. 1–43.

1040   doi:10.1895/wormbook.1.164.1

1041   29.   Haroon S, Li A, Weinert JL, Fritsch C, Ericson NG, Alexander-Floyd J, et al. Multiple

1042   Molecular Mechanisms Rescue mtDNA Disease in C. elegans. Cell Rep. Elsevier B.V.;

1043   2018;22: 3115–3125. doi:10.1016/j.celrep.2018.02.099

1044   30.   Lord CEN, Gunawardena AHLAN. Programmed cell death in C. elegans, mammals and

1045   plants. European Journal of Cell Biology. 2012. pp. 603–613.

1046   doi:10.1016/j.ejcb.2012.02.002

1047   31.   Jeong SY, Seol DW. The role of mitochondria in apoptosis. Journal of Biochemistry and

1048   Molecular Biology. 2008. pp. 11–22. doi:10.5483/bmbrep.2008.41.1.011

1049   32.   Estaquier J, Vallette F, Vayssiere JL, Mignotte B. The mitochondrial pathways of

1050   apoptosis. Adv Exp Med Biol. 2012;942: 157–183. doi:10.1007/978-94-007-2869-1_7

1051   33.   Bhola PD, Letai A. Mitochondria-Judges and Executioners of Cell Death Sentences.

1052   Molecular Cell. Cell Press; 2016. pp. 695–704. doi:10.1016/j.molcel.2016.02.019

1053   34.   Tower J. Programmed cell death in aging. Ageing Research Reviews. Elsevier Ireland Ltd;

1054   2015. pp. 90–100. doi:10.1016/j.arr.2015.04.002

1055   35.   Larsson N-G. Somatic Mitochondrial DNA Mutations in Mammalian Aging. Annu Rev

1056   Biochem. Annual Reviews; 2010;79: 683–706. doi:10.1146/annurev-biochem-060408-

1057   093701

1058   36.   Payne BAI, Chinnery PF. Mitochondrial dysfunction in aging: Much progress but many

1059   unresolved questions. Biochim Biophys Acta. 2015;1847: 1347–53.

1060   doi:10.1016/j.bbabio.2015.05.022

1061   37.   Kauppila TES, Kauppila JHK, Larsson NG. Mammalian Mitochondria and Aging: An

1062   Update. Cell Metabolism. Cell Press; 2017. pp. 57–71. doi:10.1016/j.cmet.2016.09.017

1063   38.   Conradt B, Wu YC, Xue D. Programmed cell death during Caenorhabditis elegans

1064   development. Genetics. Genetics; 2016;203: 1533–1562.

1065   doi:10.1534/genetics.115.186247

1066   39.   Gumienny TL, Lambie E, Hartwieg E, Horvitz HR, Hengartner MO. Genetic control of

1067   programmed cell death in the Caenorhabditis elegans hermaphrodite germline.

1068   Development. 1999;126: 1011–1022. doi:10.5167/uzh-1041

1069   40.   Baum JS, St. George JP, McCall K. Programmed cell death in the germline. Seminars in

71

1070   Cell and Developmental Biology. Elsevier Ltd; 2005. pp. 245–259.

1071   doi:10.1016/j.semcdb.2004.12.008

1072 41. Jaramillo-Lambert A, Ellefson M, Villeneuve AM, Engebrecht JA. Differential timing of S

1073   phases, X chromosome replication, and meiotic prophase in the C. elegans germ line. Dev

1074   Biol. Academic Press Inc.; 2007;308: 206–221. doi:10.1016/j.ydbio.2007.05.019

1075 42. Hafner A, Bulyk ML, Jambhekar A, Lahav G. The multiple mechanisms that regulate p53

1076   activity and cell fate. Nature Reviews Molecular Cell Biology. Nature Publishing Group;

1077   2019. pp. 199–210. doi:10.1038/s41580-019-0110-x

1078 43. Derry WB, Putzke AP, Rothman JH. Caenorhabditis elegans p53: Role in apoptosis,

1079   meiosis, and stress resistance. Science (80-). 2001;294: 591–595.

1080   doi:10.1126/science.1065486

1081 44. Huang W, Jiang T, Choi W, Qi S, Pang Y, Hu Q, et al. Mechanistic insights into CED-4-

1082   mediated activation of CED-3. Genes Dev. Genes Dev; 2013;27: 2039–2048.

1083   doi:10.1101/GAD.224428.113

1084 45. Seshagiri S, Miller LK. Caenorhabditis elegans CED-4 stimulates CED-3 processing and

1085   CED-3-induced. Curr Biol. Cell Press; 1997;7: 455–460. doi:10.1016/S0960-

1086   9822(06)00216-8

1087 46. Tsang WY, Lemire BD. Stable heteroplasmy but differential inheritance of a large

1088   mitochondrial DNA deletion in nematodes. Biochem Cell Biol. 2002;80: 645–654.

1089   doi:10.1139/o02-135

1090 47. Lemire B. Mitochondrial genetics. WormBook. 2005; doi:10.1895/wormbook.1.25.1

1091 48. Van Der Bliek AM, Sedensky MM, Morgan PG. Cell biology of the mitochondrion.

1092   Genetics. Genetics Society of America; 2017;207: 843–871.

1093   doi:10.1534/genetics.117.300262

1094   49.   Sousa JS, D'Imprima E, Vonck J. Mitochondrial respiratory chain complexes. Subcellular

1095   Biochemistry. Springer New York; 2018. pp. 167–227. doi:10.1007/978-981-10-7757-9_7

1096   50.   Baradaran R, Berrisford JM, Minhas GS, Sazanov LA. Crystal structure of the entire

1097   respiratory complex i. Nature. Nature; 2013;494: 443–448. doi:10.1038/nature11871

1098   51.   Song Z, Laleve A, Vallières C, McGeehan JE, Lloyd RE, Meunier B. Human Mitochondrial

1099   Cytochrome b Variants Studied in Yeast: Not All Are Silent Polymorphisms. Hum Mutat.

1100   John Wiley and Sons Inc.; 2016;37: 933–941. doi:10.1002/humu.23024

1101   52.   Gartner A, Boag PR, Blackwell TK. Germline survival and apoptosis. WormBook : the

1102   online review of C. elegans biology. 2008. pp. 1–20. doi:10.1895/wormbook.1.145.1

1103   53.   Cohen GM. Caspases: The executioners of apoptosis. Biochemical Journal. Portland Press

1104   Ltd; 1997. pp. 1–16. doi:10.1042/bj3260001

1105   54.   Shaham S, Reddien PW, Davies B, Horvitz HR. Mutational Analysis of the Caenorhabditis

1106   elegans Cell-Death Gene ced-3. Genetics. 1999;153.

1107   55.   Jeong PY, Kumar A, Joshi PM, Rothman JH. Intertwined Functions of Separase and

1108   Caspase in Cell Division and Programmed Cell Death. Sci Rep. Nature Research; 2020;10.

1109   doi:10.1038/s41598-020-63081-w

1110   56.   Denning DP, Hatch V, Horvitz HR. Both the Caspase CSP-1 and a Caspase-Independent

1111   Pathway Promote Programmed Cell Death in Parallel to the Canonical Pathway for

1112   Apoptosis in Caenorhabditis elegans. PLoS Genet. 2013;9.

1113   doi:10.1371/journal.pgen.1003341

1114   57.   Shaham S. Identification of multiple Caenorhabditis elegans caspases and their potential

1115   roles in proteolytic cascades. J Biol Chem. 1998;273: 35109–35117.

1116   doi:10.1074/jbc.273.52.35109

1117   58.   King SD, Gray CF, Song L, Nechushtai R, Gumienny TL, Mittler R, et al. The cisd gene

1118   family regulates physiological germline apoptosis through ced-13 and the canonical cell

1119   death pathway in Caenorhabditis elegans. Cell Death Differ. Nature Publishing Group;

1120   2019;26: 162–178. doi:10.1038/s41418-018-0108-5

1121   59.   Schumacher B, Schertel C, Wittenburg N, Tuck S, Mitani S, Gartner A, et al. C. elegans

1122   ced-13 can promote apoptosis and is induced in response to DNA damage. Cell Death

1123   Differ. Nature Publishing Group; 2005;12: 153–161. doi:10.1038/sj.cdd.4401539

1124   60.   Fairlie WD, Perugini MA, Kvansakul M, Chen L, Huang DCS, Colman PM. CED-4 forms a 2 :

1125   2 heterotetrameric complex with CED-9 until specifically displaced by EGL-1 or CED-13.

1126   Cell Death Differ. 2006;13: 426–434. doi:10.1038/sj.cdd.4401762

1127   61.   Conradt B, Xue D. Programmed cell death. WormBook : the online review of C. elegans

1128   biology. 2005. pp. 1–13. doi:10.1895/wormbook.1.32.1

1129   62.   Wu D, Chai Y, Zhu Z, Li W, Ou G, Li W. CED-10-WASP-Arp2/3 signaling axis regulates

1130   apoptotic cell corpse engulfment in C. elegans. Dev Biol. Academic Press Inc.; 2017;428:

1131   215–223. doi:10.1016/j.ydbio.2017.06.005

1132   63.   Kinchen JM, Cabello J, Kilngele D, Wong K, Felchtinger R, Schnabel H, et al. Two pathways

1133   converge at CED-10 to mediate actin rearrangement and corpse removal in C. elegans.

1134   Nature. 2005;434: 93–99. doi:10.1038/nature03263

1135   64.   Hochreiter-Hufford A, Ravichandran KS. Clearing the dead: Apoptotic cell sensing,

1136   recognition, engulfment, and digestion. Cold Spring Harb Perspect Biol. 2013;5.

1137   doi:10.1101/cshperspect.a008748

1138   65.   Wang X, Yang C. Programmed cell death and clearance of cell corpses in Caenorhabditis

1139   elegans. Cellular and Molecular Life Sciences. Birkhauser Verlag AG; 2016. pp. 2221–

1140   2236. doi:10.1007/s00018-016-2196-z

1141   66.   Reddien PW, Horvitz HR. THE ENGULFMENT PROCESS OF PROGRAMMED CELL DEATH IN

1142   *CAENORHABDITIS ELEGANS*. Annu Rev Cell Dev Biol. Annual Reviews; 2004;20: 193–221.

1143   doi:10.1146/annurev.cellbio.20.022003.114619

1144   67.   Hoeppner DJ, Hengartner MO, Schnabel R. Engulfment genes cooperate with ced-3 to

1145   promote cell death in Caenorhabditis elegans. Nature. Nature Publishing Group;

1146   2001;412: 202–206. doi:10.1038/35084103

1147   68.   Geng X, Zhou QH, Kage-Nakadai E, Shi Y, Yan N, Mitani S, et al. Caenorhabditis elegans

1148   caspase homolog CSP-2 inhibits CED-3 autoactivation and apoptosis in germ cells. Cell

1149   Death Differ. 2009;16: 1385–1394. doi:10.1038/cdd.2009.88

1150   69.   Yang X, Chang HY, Baltimore D. Essential role of CED-4 oligomerization in CED-3

1151   activation and apoptosis. Science (80-). American Association for the Advancement of

1152   Science; 1998;281: 1355–1357. doi:10.1126/science.281.5381.1355

1153   70.   Parsons MJ, Green DR. Mitochondria in cell death. Essays Biochem. 2010;47: 99–114.

1154   doi:10.1042/BSE0470099

1155   71.   Harman D. Free radical theory of aging. Mutat Res. 1992;275: 257–266.

1156   doi:10.1016/0921-8734(92)90030-S

1157   72.   HARMAN D. Aging: a theory based on free radical and radiation chemistry. J Gerontol.

1158   1956;11: 298–300. doi:10.1093/geronj/11.3.298

1159   73.   Szczepanowska K, Trifunovic A. Origins of mtDNA mutations in ageing. Essays in

1160   Biochemistry. Portland Press Ltd; 2017. pp. 325–337. doi:10.1042/EBC20160090

1161   74.   Bratic A, Larsson N-G. The role of mitochondria in aging. J Clin Invest. 2013;123: 951–957.

1162   doi:10.1172/JCI64125

1163   75.   Ziegler D V., Wiley CD, Velarde MC. Mitochondrial effectors of cellular senescence:

1164   Beyond the free radical theory of aging. Aging Cell. Blackwell Publishing Ltd; 2015. pp. 1–

1165   7. doi:10.1111/acel.12287

1166   76.   Kimble J, Crittenden SL. Germline proliferation and its control. WormBook : the online

1167   review of C. elegans biology. 2005. pp. 1–14. doi:10.1895/wormbook.1.13.1

1168   77.   Yoon DS, Alfhili MA, Friend K, Lee MH. MPK-1/ERK regulatory network controls the

1169   number of sperm by regulating timing of sperm-oocyte switch in C. elegans germline.

1170   Biochem Biophys Res Commun. Elsevier B.V.; 2017;491: 1077–1082.

1171   doi:10.1016/j.bbrc.2017.08.014

1172   78.   Angeles-Albores D, Leighton DHW, Tsou T, Khaw TH, Antoshechkin I, Sternberg PW. The

1173   Caenorhabditis elegans female-like state: Decoupling the transcriptomic effects of aging

1174   and sperm status. G3 Genes, Genomes, Genet. Genetics Society of America; 2017;7:

1175   2969–2977. doi:10.1534/g3.117.300080

1176   79.   Kujoth CC, Hiona A, Pugh TD, Someya S, Panzer K, Wohlgemuth SE, et al. Medicine:

1177   Mitochondrial DNA mutations, oxidative stress, and apoptosis in mammalian aging.

1178   Science (80-). American Association for the Advancement of Science; 2005;309: 481–

1179   484. doi:10.1126/science.1112125

1180   80.   Beanan MJ, Strome S. Characterization of a germ-line proliferation mutation in C.

1181   elegans. Development. 1992;116.

1182   81.   Barton MK, Schedl TB, Kimble J. Gain-of-function mutations of fem-3, a sex-

1183   determination gene in Caenorhabditis elegans. Genetics. 1987;115: 107–119.

1184   82.   Bartke A. Insulin and aging. Cell Cycle. Taylor and Francis Inc.; 2008. pp. 3338–3343.

1185   doi:10.4161/cc.7.21.7012

1186   83.   Anisimov VN, Bartke A. The key role of growth hormone-insulin-IGF-1 signaling in aging

1187   and cancer. Critical Reviews in Oncology/Hematology. 2013. pp. 201–223.

1188   doi:10.1016/j.critrevonc.2013.01.005

1189   84.   Piper MDW, Selman C, McElwee JJ, Partridge L. Separating cause from effect: how does

1190   insulin/IGF signalling control lifespan in worms, flies and mice? J Intern Med. John Wiley

1191   & Sons, Ltd; 2008;263: 179–191. doi:10.1111/J.1365-2796.2007.01906.X

1192   85.   Kenyon C, Chang J, Gensch E, Rudner A, Tabtiang R. A C. elegans mutant that lives twice

1193   as long as wild type. Nature. 1993;366: 461–464. doi:10.1038/366461a0

1194   86.   Tatar M, Kopelman A, Epstein D, Tu M-P, Yin C-M, Garofalo RS. A Mutant Drosophila

1195   Insulin Receptor Homolog That Extends Life-Span and Impairs Neuroendocrine Function.

1196   Science (80-). American Association for the Advancement of Science; 2001;292: 107–

1197   110. doi:10.1126/SCIENCE.1057987

1198   87.   Blüher M, Kahn BB, Kahn CR. Extended Longevity in Mice Lacking the Insulin Receptor in

1199   Adipose Tissue. Science (80-). American Association for the Advancement of Science;

1200   2003;299: 572–574. doi:10.1126/SCIENCE.1078223

1201   88.   Gitschlag BL, Tate AT, Patel MR. Nutrient status shapes selfish mitochondrial genome

1202   dynamics across different levels of selection. Elife. eLife Sciences Publications Ltd;

1203   2020;9: 1–27. doi:10.7554/ELIFE.56686

1204   89.   Apfeld J, O'Connor G, McDonagh T, DiStefano PS, Curtis R. The AMP-activated protein

1205   kinase AAK-2 links energy levels and insulin-like signals to lifespan in C. elegans. Genes

1206   Dev. Cold Spring Harbor Laboratory Press; 2004;18: 3004–3009.

1207   doi:10.1101/gad.1255404

1208   90.   Miyadera H, Kano K, Miyoshi H, Ishii N, Hekimi S, Kita K. Quinones in long-lived clk-1

1209   mutants of Caenorhabditis elegans. FEBS Lett. No longer published by Elsevier; 2002;512:

1210   33–37. doi:10.1016/S0014-5793(02)02282-2

1211   91.   Miyadera H, Amino H, Hiraishi A, Taka H, Murayama K, Miyoshi H, et al. Altered Quinone

1212   Biosynthesis in the Long-lived clk-1Mutants of Caenorhabditis elegans. J Biol Chem.

1213   Elsevier; 2001;276: 7713–7716. doi:10.1074/JBC.C000889200

1214   92.   Kirby CS, Patel MR. Elevated mitochondrial DNA copy number found in ubiquinone-

1215   deficient clk-1 mutants is not rescued by ubiquinone precursor 2-4-dihydroxybenzoate.

1216   Mitochondrion. Elsevier B.V.; 2021;58: 38–48. doi:10.1016/j.mito.2021.02.001

1217   93.   Charmpilas N, Tavernarakis N. Mitochondrial maturation drives germline stem cell

1218   differentiation in Caenorhabditis elegans. Cell Death Differ. Springer Nature; 2020;27:

1219   601–617. doi:10.1038/s41418-019-0375-9

1220   94.   Folmes CDL, Ma H, Mitalipov S, Terzic A. Mitochondria in pluripotent stem cells:

1221   Stemness regulators and disease targets. Current Opinion in Genetics and Development.

1222   Elsevier Ltd; 2016. pp. 1–7. doi:10.1016/j.gde.2016.02.001

1223   95.   Floros VI, Pyle A, DIetmann S, Wei W, Tang WWC, Irie N, et al. Segregation of

1224   mitochondrial DNA heteroplasmy through a developmental genetic bottleneck in human

1225   embryos. Nat Cell Biol. 2018; 144–151. doi:10.1038/s41556-017-0017-8

1226 96. Zhang H, Burr SP, Chinnery PF. The mitochondrial DNA genetic bottleneck: Inheritance

1227   and beyond. Essays in Biochemistry. Portland Press Ltd; 2018. pp. 225–234.

1228   doi:10.1042/EBC20170096

1229 97. Wai T, Teoli D, Shoubridge EA. The mitochondrial DNA genetic bottleneck results from

1230   replication of a subpopulation of genomes. Nat Genet. 2008; 1484–1488.

1231   doi:10.1038/ng.258

1232 98. Liau WS, Gonzalez-Serricchio AS, Deshommes C, Chin K, LaMunyon CW. A persistent

1233   mitochondrial deletion reduces fitness and sperm performance in heteroplasmic

1234   populations of C. elegans. BMC Genet. BioMed Central; 2007;8: 1–11. doi:10.1186/1471-

1235   2156-8-8

1236 99. Zhu Z, Han X, Wang Y, Liu W, Lu Y, Xu C, et al. Identification of Specific Nuclear Genetic

1237   Loci and Genes That Interact With the Mitochondrial Genome and Contribute to

1238   Fecundity in Caenorhabditis elegans. Front Genet. Frontiers; 2019;10: 28.

1239   doi:10.3389/fgene.2019.00028

1240 100. Levin L, Blumberg A, Barshad G, Mishmar D. Mito-nuclear co-evolution: The positive and

1241   negative sides of functional ancient mutations. Front Genet. Frontiers Media S.A.;

1242   2014;5: 448. doi:10.3389/fgene.2014.00448

1243 101. Paliwal S, Fiumera AC, Fiumera HL. Mitochondrial-nuclear epistasis contributes to

1244   phenotypic variation and coadaptation in natural isolates of saccharomyces cerevisiae.

1245   Genetics. Genetics Society of America; 2014;198: 1251–1265.

1246   doi:10.1534/genetics.114.168575

1247   102. Zhu CT, Ingelmo P, Rand DM. G×G×E for Lifespan in Drosophila: Mitochondrial, Nuclear,

1248   and Dietary Interactions that Modify Longevity. PLoS Genet. Public Library of Science;

1249   2014;10. doi:10.1371/journal.pgen.1004354

1250   103. Meiklejohn CD, Holmbeck MA, Siddiq MA, Abt DN, Rand DM, Montooth KL. An

1251   Incompatibility between a Mitochondrial tRNA and Its Nuclear-Encoded tRNA Synthetase

1252   Compromises Development and Fitness in Drosophila. PLoS Genet. Public Library of

1253   Science; 2013;9. doi:10.1371/journal.pgen.1003238

1254   104. Dingley SD, Polyak E, Ostrovsky J, Srinivasan S, Lee I, Rosenfeld AB, et al. Mitochondrial

1255   DNA Variant in COX1 Subunit Significantly Alters Energy Metabolism of Geographically

1256   Divergent Wild Isolates in Caenorhabditis elegans. J Mol Biol. 2014;426: 2199–2216.

1257   doi:10.1016/j.jmb.2014.02.009

1258   105. Yee C, Yang W, Hekimi S. The intrinsic apoptosis pathway mediates the pro-longevity

1259   response to mitochondrial ROS in C. elegans. Cell. PMC Canada manuscript submission;

1260   2014;157: 897. doi:10.1016/J.CELL.2014.02.055

1261   106. H H, C K. Signals from the reproductive system regulate the lifespan of C. elegans.

1262   Nature. Nature; 1999;399: 362–366. doi:10.1038/20694

1263   107. L D, CW A, S K. New insights into apoptosome structure and function. Cell Death Differ.

1264   Cell Death Differ; 2018;25: 1194–1208. doi:10.1038/S41418-017-0025-Z

1265   108. S Y, X Y, JM A, JE H, SJ L, CW A. The holo-apoptosome: activation of procaspase-9 and

1266   interactions with caspase-3. Structure. Structure; 2011;19: 1084–1096.

1267   doi:10.1016/J.STR.2011.07.001

1268   109.   Zermati Y, Mouhamad S, Stergiou L, Besse B, Galluzzi L, Boehrer S, et al. Nonapoptotic

1269   Role for Apaf-1 in the DNA Damage Checkpoint. Mol Cell. Cell Press; 2007;28: 624–637.

1270   doi:10.1016/j.molcel.2007.09.030

1271   110.   Ferraro E, Pesaresi MG, De Zio D, Cencioni MT, Gortat A, Cozzolino M, et al. Apaf1 plays a

1272   pro-survival role by regulating centrosome morphology and function. J Cell Sci. 2011;124:

1273   3450–3463. doi:10.1242/jcs.086298

1274   111.   Liu WH, Lin YL, Wang JP, Liou W, Hou RF, Wu YC, et al. Restriction of vaccinia virus

1275   replication by a ced-3 and ced-4-dependent pathway in Caenorhabditis elegans. Proc

1276   Natl Acad Sci U S A. National Academy of Sciences; 2006;103: 4174–4179.

1277   doi:10.1073/pnas.0506442103

1278   112.   Wang G, Sun L, Reina CP, Song I, Gabel C V., Driscoll M. CED-4 CARD domain residues can

1279   modulate non-apoptotic neuronal regeneration functions independently from apoptosis.

1280   Sci Rep. 2019;9: 13315. doi:10.1038/s41598-019-49633-9

1281   113.   Chaudhary D, O'Rourke K, Chinnaiyan AM, Dixit VM. The Death Inhibitory Molecules CED-

1282   9 and CED-4L Use a Common Mechanism to Inhibit the CED-3 Death Protease. J Biol

1283   Chem. Elsevier; 1998;273: 17708–17712. doi:10.1074/JBC.273.28.17708

1284   114.   Mack HID, Zhang P, Fonslow BR, Yates JR. The protein kinase MBK-1 contributes to

1285   lifespan extension in daf-2 mutant and germline-deficient Caenorhabditis elegans. Aging

1286   (Albany NY). Impact Journals LLC; 2017;9: 1414–1432. doi:10.18632/aging.101244

1287   115.   Libina N, Berman JR, Kenyon C. Tissue-Specific Activities of C. elegans DAF-16 in the

1288   Regulation of Lifespan. Cell. Cell Press; 2003;115: 489–502. doi:10.1016/S0092-

1289   8674(03)00889-4

1290   116.   Lapierre LR, Hansen M. Lessons from C. elegans: signaling pathways for longevity. Trends

1291   Endocrinol Metab. Elsevier Current Trends; 2012;23: 637–644.

1292   doi:10.1016/J.TEM.2012.07.007

1293   117.   A A. Regulation of longevity by the reproductive system. Exp Gerontol. Exp Gerontol;

1294   2013;48: 596–602. doi:10.1016/J.EXGER.2012.09.009

1295   118.   Branicky R, Bénard C, Hekimi S. clk-1, mitochondria, and physiological rates. BioEssays.

1296   2000. pp. 48–56. doi:10.1002/(SICI)1521-1878(200001)22:1<48::AID-BIES9>3.0.CO;2-F

1297   119.   Hekimi S, Guarente L. Genetics and the specificity of the aging process. Science. 2003. pp.

1298   1351–1354. doi:10.1126/science.1082358

1299   120.   Blackwell TK, Steinbaugh MJ, Hourihan JM, Ewald CY, Isik M. SKN-1/Nrf, stress responses,

1300   and aging in Caenorhabditis elegans. Free Radic Biol Med. Pergamon; 2015;88: 290–301.

1301   doi:10.1016/J.FREERADBIOMED.2015.06.008

1302   121.   Youle RJ, Van Der Bliek AM. Mitochondrial fission, fusion, and stress. Science. American

1303   Association for the Advancement of Science; 2012. pp. 1062–1065.

1304   doi:10.1126/science.1219855

1305   122.   Twig G, Elorza A, Molina AJA, Mohamed H, Wikstrom JD, Walzer G, et al. Fission and

1306   selective fusion govern mitochondrial segregation and elimination by autophagy. EMBO

1307   J. 2008;27: 433–446. doi:10.1038/sj.emboj.7601963

1308   123.   Stiernagle T. Maintenance of C. elegans. WormBook : the online review of C. elegans

1309   biology. 2006. pp. 1–11. doi:10.1895/wormbook.1.101.1

1310   124.   C. elegans Deletion Mutant Consortium. large-scale screening for targeted knockouts in

1311   the Caenorhabditis elegans genome. G3 (Bethesda). 2012;2: 1415–25.

1312   doi:10.1534/g3.112.003830

1313   125.   Li H, Durbin R. Fast and accurate short read alignment with Burrows–Wheeler transform.

1314   Bioinformatics. Oxford Academic; 2009;25: 1754–1760.

1315   doi:10.1093/BIOINFORMATICS/BTP324

1316   126.   Li H, Handsaker B, Wysoker A, Fennell T, Ruan J, Homer N, et al. The Sequence

1317   Alignment/Map format and SAMtools. Bioinformatics. Oxford Academic; 2009;25: 2078–

1318   2079. doi:10.1093/BIOINFORMATICS/BTP352

1319   127.   Koboldt DC, Chen K, Wylie T, Larson DE, McLellan MD, Mardis ER, et al. VarScan: variant

1320   detection in massively parallel sequencing of individual and pooled samples.

1321   Bioinformatics. Oxford Academic; 2009;25: 2283–2285.

1322   doi:10.1093/BIOINFORMATICS/BTP373

1323

1324